


Review

In-Situ Fabrication, Microstructure and Mechanical Performance of Nano Iron-Rich Precipitate Reinforced Cu and Cu Alloys

Zongxuan Li ¹, Kaixuan Chen ^{1,*} , Xiaohua Chen ², Yuzhi Zhu ¹, Mingwen Chen ³, Yanlin Wang ^{1,2}, Jiangxu Shen ¹, Jiayun Shi ¹ and Zidong Wang ^{1,*}

¹ School of Materials Science and Engineering, University of Science and Technology Beijing, Beijing 100083, China

² State Key Laboratory for Advanced Metals and Materials, University of Science and Technology Beijing, Beijing 100083, China

³ School of Mathematics and Physics, University of Science and Technology Beijing, Beijing 100083, China

* Correspondence: chenxustb@126.com (K.C.); wangzd@mater.ustb.edu.cn (Z.W.); Tel.: +86-010-62333152 (K.C. & Z.W.)

Abstract: In this paper, the research progress on the strengthening of copper and copper alloy is reviewed. The research shows that traditional strengthening methods are often accompanied by the decrease of plasticity, and there are limitations in size, cost, and other aspects in the process. The in-situ nanoparticle strengthening and plasticizing technology proposed in recent years can avoid the above problems. In this paper, the idea of in-situ nanoparticle strengthening is introduced to realize the simultaneous enhancement of strength and ductility of as-cast pure copper and tin bronze alloys. The effects of in-situ precipitation of iron-rich nanoparticles on the microstructure, and mechanical properties of different copper alloy systems, are systematically elucidated based on the former characterization and mechanical testing results. The results show that the in-situ introduction of iron-rich nanoparticles in the copper systems induces the formation of a nano precipitate-fine grain (NPF) structure, which greatly improves the strength and ductility of copper alloys. The evolution of size, distribution, number density, morphology evolution in iron-rich nanoparticles, and the formation mechanism of NPF structure, as well as the mechanism of NPF strengthening and toughening, are summarized. An industrial-applicable casting process is proposed to prepare bulk NPF structured copper alloys with complex shape, high strength, and high ductility.

Keywords: copper alloy; in-situ nanoparticle; grain refinement; strengthening; plasticizing



Citation: Li, Z.; Chen, K.; Chen, X.; Zhu, Y.; Chen, M.; Wang, Y.; Shen, J.; Shi, J.; Wang, Z. In-Situ Fabrication, Microstructure and Mechanical Performance of Nano Iron-Rich Precipitate Reinforced Cu and Cu Alloys. *Metals* **2022**, *12*, 1453. <https://doi.org/10.3390/met12091453>

Academic Editor:
Carlos Garcia-Mateo

Received: 20 July 2022

Accepted: 22 August 2022

Published: 30 August 2022

Publisher's Note: MDPI stays neutral with regard to jurisdictional claims in published maps and institutional affiliations.



Copyright: © 2022 by the authors. Licensee MDPI, Basel, Switzerland. This article is an open access article distributed under the terms and conditions of the Creative Commons Attribution (CC BY) license (<https://creativecommons.org/licenses/by/4.0/>).

1. Introduction

Metallic materials such as steels, copper and copper alloys, aluminum and aluminum alloys, magnesium and magnesium alloys, are widely used in shipbuilding, automobile, aircraft, and other manufacturing industries. With the rapid development of modern science and technology, the requirements for metal materials are getting higher and higher, which requires the comprehensive improvement of material properties [1]. Improving the strength of metal materials, while avoiding the loss of other properties, including elongation, conductivity, and high temperature stability, is the future direction in the materials area. The mechanical properties of metallic materials are mainly determined by their microstructure, so the comprehensive mechanical properties can be improved by optimizing the microstructure of metallic materials.

Grain refinement and second phase precipitation are the key methods to optimize microstructure and are widely used in strengthening. For grain-refining strengthening, according to the Hall-Petch relation, the strength of polycrystalline materials increases with the decrease of grain size [2,3], especially for ultrafine grain materials (grain size of

~1 μm), which achieve ultrahigh strength at room temperature and ultrahigh plasticity at high temperature [4]. Nanocrystalline and ultrafine grain materials can be prepared by severe plastic deformation (SPD), such as equal channel angular pressing (ECAP) [5–9] and high-pressure torsion (HPT) [10–12]. These methods refine the grain size of metallic materials to 100–1000 nm, or even less than 100 nm. However, SPD methods only prepare millimeter-scale samples and are subjected to shape limitations, e.g., only cylindrical, or cubic shape is available.

The inert gas condensation in-situ compression and mechanical alloying methods have been applied to prepare large-scale bulk nanocrystalline and ultrafine grain materials. However, the process equipment of inert gas condensation in-situ compression method is complex and with low production efficiency, and the prepared materials are always with micro pores. Mechanical alloying is prone to cause stress, impurities, pollution, and oxidation. In contrast, in the solidification process, the combination of deep undercooling, and deep undercooling with other grain refinement methods, avoid the shortcomings of the above preparation process. Deep undercooling significantly accelerates the cooling rate and solidification rate. Using this method to prepare bulk nanocrystalline and ultrafine grain materials not only obtain bulk nanocrystals with clean interface and no micro pores, but also greatly reduces the process and cost. The formation of ultrafine grains in rapidly solidified alloys is the result of a high nucleation rate at deep undercooling [13]. Although the microstructure of the alloy is refined by increasing the solidification rate, and even the solidification microstructure of the alloy can be reduced to nano-sized scale, the rapid solidification is realized under extreme experimental conditions, which is not applicable in the industrial production of bulk metal materials due to the limitation in size [14]. Therefore, the preparation of bulk ultrafine grain materials is still a problem. From the perspective of improving the comprehensive properties of materials, when the grain size of metallic materials is greater than 1 μm , grain refinement improves the strength of the material without causing the decrease of ductility. When the grain size of metal materials reaches the nanometer scale (~1 μm), further grain refinement is accompanied by the deterioration of ductility and toughness [1,15]. Besides, the soften or strength decreasing occurs in metals as the grain size is refined to a certain critical size (e.g., 10–15 nm for pure copper) [16].

Second phase strengthening is another important strengthening method for metallic materials. Industrial metallic materials such as steels, copper alloys, aluminum alloys, etc., are mainly strengthened with micron and submicron second phase particles. This kind of micron and submicron second phase particles always reduce the ductility in the meantime. The deterioration of ductility by high concentration of ceramic-type strengthening particles is particularly obvious [17–24]. According to the Orowan-Ashb model, the refinement of the second phase is conducive to the simultaneous improvement of the strength and ductility of materials [25–28]. Especially when the second phase is refined to the nanoscale, the interface between the second phase particles and the matrix maintains a coherent or semi-coherent relationship, and the interaction mode between dislocation and the second phase become favorable; that is, in the process of hindering the movement of dislocations, some dislocations enter into the particle along the coherent interface, to weaken the dislocation pile-up and improve the strength and toughness of the alloy [29]. Therefore, nanoparticle strengthening becomes a favorable strategy to improve the performance of metallic materials. It is popular to enhance the strength of metallic materials by using nano-sized second phase particles [25,30–32]. If the nano-reinforced phase with a coherent or semi-coherent interface is more evenly distributed and with higher number density in the matrix, the strengthening effect is able to be improved along with the less weakening to the elongation.

In order to obtain second phase strengthening particles with appropriate size (favorably in nanometer scale), shape, particle spacing and spatial distribution, powder metallurgy, internal oxidation, and spray deposition methods, are often used to prepare dispersion strengthening alloys [19,33–36]. However, these methods are difficult to be applied in mass production due to their complex preparation process, high cost, and energy

consumption [19]. Moreover, mechanical alloying materials in the subsequent high temperature heat treatment process are accompanied by the generation of holes, and significantly deteriorate the performance of the material [37].

In addition to fine grain strengthening and second phase strengthening, solid solution strengthening and dislocation strengthening are also important strengthening methods of metals and alloys. These methods are all through the introduction of internal point line defects or interfaces in metal materials, which interact with dislocations in the deformation process to yield the strengthening effect. However, these internal defects impede the movement of dislocations and inevitably cause the reduction of ductility and the improvement of brittleness, and even deteriorate the comprehensive mechanical properties of metallic materials [38–41]. The optimal combination of strength and ductility is still a challenge to be obtained for metallic materials.

The strategy of in-situ nanoparticle strengthening was proposed by Wang et al. [29–32,42–50] to achieve the simultaneous enhancement of strength and ductility in metal materials. In other words, through the addition of trace Fe and/or Co elements in the smelting process of copper alloy, well-dispersed nano-sized iron-rich precipitates are generated in the casting process. Meanwhile, the matrix grains are refined to 1–100 μm , and the nano precipitate-fine grain (NPF) structure is hence produced. The strength and ductility of copper alloy are both improved by the synergistic effect of fine grains and inside coherent or semi-coherent iron-rich nanoparticles. This NPF structure is prepared directly by the solidification process, which is applicable in mass production of bulk metallic materials with complex shapes.

In this paper, with the background statement on dispersion strengthening and (ultra) fine grain strengthening of copper alloys, the concept of in-situ nanoparticle strengthening and the idea of strengthening and plasticizing by NPF structure are introduced, and the preparation, microstructural, and mechanical characteristics of in-situ nanoparticle reinforced copper alloys, are summarized. This paper sheds light on the significance of in-situ nano precipitate reinforced Cu and Cu alloys and the application of NPF strategy on strengthening and plasticizing, which provide guidance for their application in more alloy systems.

2. Strengthening Method of Copper Alloy

The microstructure of a metallic material determines its properties and hence its application; hence, microstructural optimization is the basis of materials development. For copper alloys, high strength and considerable plasticity can ensure its wide, durable, and safe service. Previous studies have shown that the traditional strengthening method often increases the strength of copper alloys, but inevitably decreases ductility. The contradiction between strength and plasticity of copper alloys is the essential problem to be urgently solved. In the past 20 years, dispersion strengthened copper alloys have become a new type of widely-used composite material, because of its excellent comprehensive physical and mechanical properties [17–19,33,34]. In addition, the preparation of ultrafine grains by severe plastic deformation (SPD) has become an important strengthening concept of copper alloys [4].

2.1. Dispersion Strengthening Copper Alloys

Dispersion strengthening alloy is a kind of composite material which adds fine and dispersed second phase particles into the metal matrix, thus hindering dislocation movement and greatly improving the strength of the matrix. Due to the low content and dispersive distribution of the second phase particles in the alloy, the alloy still has the characteristics of high strength, high hardness, high conductivity, and high softening temperature of copper matrix. Dispersion strengthening copper alloys are composite materials with excellent comprehensive physical and mechanical properties. Therefore, it is widely used in large-scale microwave tube structure, conductive materials, conversion switches, integrated circuit lead frame, contacts, and spot-welding electrodes, etc. [51].

For copper matrix, most of the dispersion strengthening particles studied are additional ceramic particles, such as Al_2O_3 , boride (TiB_2), carbide (SiC , TiC), and nitride, and the size of strengthening particles reported in the literature for industrial application is mostly micron or submicron [18,19,33,34]. Due to the large size of the introduced particles and the poor wettability with the matrix, the interface between the second phase and the matrix is non-coherent. In the process of dislocation movement, due to the failure to pass through the second phase particles, the accumulation occurs at the interface, resulting in stress concentration. This situation enhances the ability of the alloy to suffer plastic deformation at the cost of sacrificing the plasticity [1,19,38]. Therefore, the introduction of these micron-sized particles significantly deteriorates the ductility, while strengthening the matrix. In order to obtain the second phase strengthening particles with appropriate size (even in nanometer scale), shape, spacing and distribution, powder metallurgy, mechanical alloying, the internal oxidation method, the sol-gel method, and the chemical precipitation method, are commonly used to prepare dispersion strengthening copper alloys.

Mechanical alloying [52] is the ball milling of different powders in a high-energy ball mill. After the collision and extrusion of the balls, the powders are repeatedly deformed, fractured, and welded, and the atoms are diffused or solid-state reacted to form alloy powders. There are two main types of composite powders prepared by the mechanical alloying method: (1) The matrix copper and ceramic particles are grinded in a high energy ball mill for a long time, so that the raw metal materials reach the close combination state at the atomic level, and the hard particles are uniformly embedded in the metal particles to obtain the composite powder; (2) The elemental powders to be alloyed are mechanically mixed according to a certain proportion, and the dispersion strengthening phase is in-situ formed through the chemical reaction during mechanical alloying. The introduction of nanoparticles by this method avoids the disadvantages of a complex preparation process, high cost, and easy agglomeration of nanoparticles, and the prepared composite powder has a good interfacial effect.

The internal oxidation method [52] applies the chemical thermal reduction reaction principle to add the unstable compound powder into the alloy powder, thence the components in the alloy react with the added compound to generate the required, more stable, reinforcement particles. Then, the mixed powder is pressed and sintered to make composite materials. So far, the development of the internal oxidation method has been relatively mature, and the comprehensive performance of its products has also been unanimously affirmed. However, some shortcomings cannot be ignored. For example, it is impossible to obtain fully dense and fully metallurgical metal-based materials by using a simple sintering process, and the comprehensive performance of the materials is further deteriorated at high temperature. Besides, the preparation process of dispersion strengthened copper matrix composites by the internal oxidation method is complex and the production cycle is long, which directly leads to high production costs, difficulty in accurately controlling the quality of products and achieving automation, and large-scale production.

Chemical precipitation [53] is mainly achieved through a chemical process. In this process, a mixture of insoluble compounds (mostly hydroxides or carbonates) is firstly precepted in the applicable metal salt solution, which then experience a reduction treatment. The latter reduction treatment results in the reduction of metal matrix, along with the associated metal retained in the form of oxides. Finally, the obtained mixed powder suffers solidification and deformation by extrusion and other processes. A fine dispersion phase is obtained by the chemical precipitation method, and the prepared dispersion strengthening copper alloys exhibit good electrical conductivity. However, due to the influence of the reduction process and raw material purity, the performance of the sintered product is always poor. The method is accompanied by a complex process, low production efficiency, and high cost.

The sol-gel method [54] is another process for the preparation of dispersion strengthening copper. After the initial $\text{Al}(\text{OH})_3$ sol is prepared by Sol-Gel technology, the reduced copper powder is added to prepared $\text{Al}_2\text{O}_3/\text{Cu}$ composite powder, and then hot pressing

sintering is carried out to obtain ultrafine Al_2O_3 dispersion strengthening copper alloys. The process is easy to control and the cost is low. The prepared dispersion strengthened copper has good strength and conductivity, high density, and good high temperature stability.

Powder metallurgy [55] is an industrial technology for preparing metallic materials, composite materials, and various types of products, by forming and sintering metal powder or using metal powder (or a mixture of metal powder and non-metal powder) as raw material. In recent years, the reinforced phase of copper matrix composites fabricated by powder metallurgy is becoming finer and finer, and it develops to nanometer level. The commonly used reinforced phases include borides, oxides, carbides, nitrides and silicides, and a series of intermediate phases such as Fe_2P and Co_2P . Powder metallurgy is the first method used to manufacture metal matrix composites. This technology possesses many advantages, e.g., it can realize various types of composites and give full play to the characteristics of each component. It is a low-cost technology to produce composite materials. Meanwhile, due to the great differences in size, shape, and physical and chemical properties between the matrix and the reinforcement, improving the wettability between the reinforcement and the matrix, and enhancing the interfacial bonding strength between the matrix and the reinforcement, the difficulty of improving the comprehensive performance of metal matrix composites remains.

In summary, the second phase particles, especially the micron-sized particles, deteriorate their ductility, while strengthening the copper and copper alloys. The strengthening effect of the highly dispersed nano-sized second phase is better than that of the micron-sized and submicron-sized second phases, and their matching relationship with the matrix is better. On the basis of maintaining the coherent and semi-coherent, it can effectively avoid the accumulation of dislocations at the particle/matrix interface, so that the dislocations either slip or partially enter into the particles to reduce the stress concentration at the interface, so that the particle/matrix interface is not easy to become a crack source, thereby improving the strength of the alloy and in the meantime ensuring its plasticity.

Therefore, it is necessary to refine the reinforced particles to the nanometer scale to significantly improve the comprehensive mechanical properties. Dispersive particles reinforced copper and copper alloys have been widely used, but there are still many problems in the preparation of copper matrix composites by means of external strengthening particles, such as uncontrollable particle size, uneven particle distribution (particles prone to segregation), poor particle/matrix interface relationship, and no obvious optimization effect on the solidification structure of the matrix itself. Moreover, the preparation of copper matrix composites by adding reinforcement has high production process requirements, long production process time, and high cost, and the existence of these problems limits the development of dispersion strengthening copper alloys.

2.2. Ultrafine Grained Copper and Copper Alloys

Grain-refining strengthening [56] is to improve strength by reducing grain size. Because the external force can be dispersed in more grains when the fine-grained copper is deformed under force, the plastic deformation is relatively uniform and the stress concentration is lower. In addition, the finer grains provide more grain boundary area and thus more zigzag of the grain boundary, which is favorable to impede crack expansion. In consequence, fine-grained copper and copper alloys have a higher strength, hardness, plasticity, and toughness, than coarse-grained ones at room temperature. Grain-refining strengthening follows the Hall-Petch relation [2,3], but cannot describe the strength of grains below 10–20 nm since such a small grain cannot carry the accumulation of dislocations. It is found that when the grain size is less than 1 μm , it can achieve ultrahigh strength at room temperature and ultrahigh plasticity at high temperature [4]. It is precisely because of the high strength and high plasticity of ultrafine grained (UFG) materials (grain size <1 μm) that its preparation has also attracted wide attention.

Severe plastic deformation (SPD) has become an important method to refine the grain structure of polycrystalline copper alloys to submicron or even nano-scale due to its

strong grain refinement ability. The common SPD methods include equal channel angular extrusion (ECAP), high pressure torsion (HPT), cumulative rolling, and multidirectional forging, and are used in copper and copper alloys [57]. ECAP [5–9] is a method for preparing bulk nanocrystalline materials by directly refining the grains through severe plastic deformation. At present, ECAP technology has become one of the most rapidly developed technologies in SPD of copper. The mechanism is that the copper specimen is intersected by two axes under a certain extrusion force, and the cross-section size is equal and forms a channel with a certain angle. The pure shear deformation occurs on the specimen under the extrusion force to achieve grain refinement. The schematic of ECAP is shown in Figure 1a.

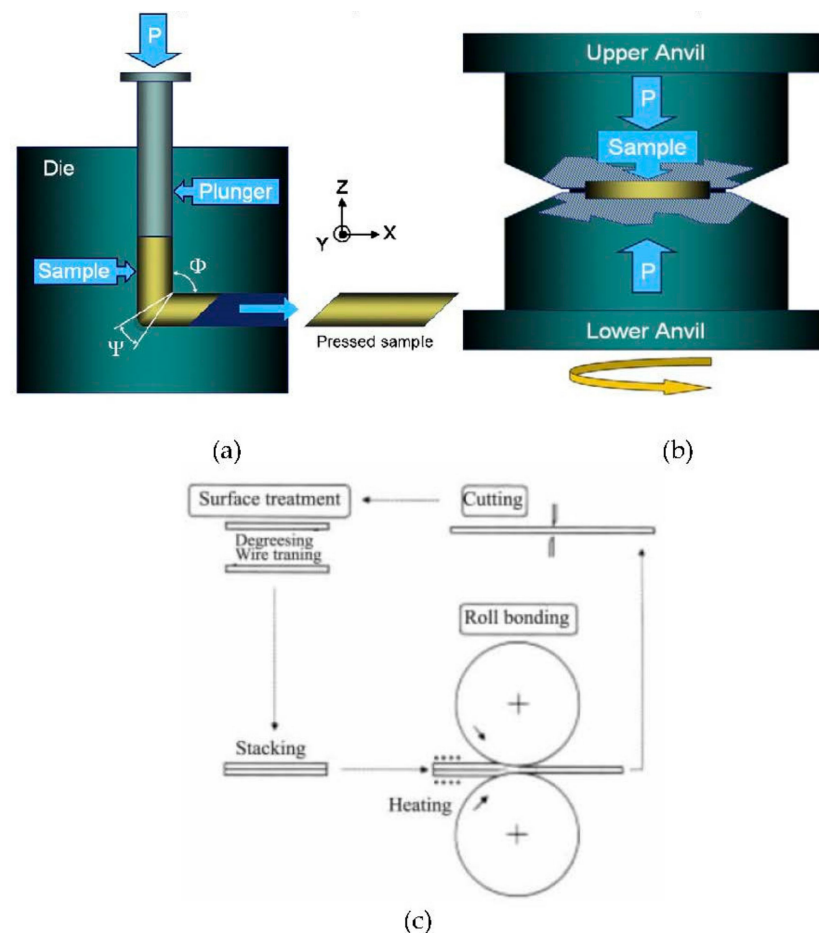


Figure 1. The schematics of (a) ECAP process including an X, Y, Z coordinate system [4]; (b) HPT process [4]; and (c) ARB process [58].

HPT [57] is a SPD process proposed and developed by Bridgman. Figure 1b is the HPT diagram of a thin disk specimen. When this device is used for deformation, the thin disc sample is applied with GPa-level high pressure to twist. Since the size of the deformed specimen does not change, a large shear strain is introduced on the outer side of the specimen, which makes the metallic material undergo SPD, and the grain size continues to decrease until ultrafine or even nano grains are formed. Due to the influence of the mold under the allowable pressure and the external pressure of the specimen, the material has shear deformation under a condition similar to the static pressure. Therefore, although the material strain is large, the specimen is not easy to break.

Accumulative roll bonding (ARB) is a deformation method proposed by Saito et al. to prepare nanostructured copper materials [58]. The continuous preparation of ultrafine-grained copper alloys is realized by using the method of cumulative rolling and large

deformation. However, in order to eliminate work hardening, edge cracking and interface recombination in the process of cumulative rolling, the rolling process must be carried out at a certain temperature, which reduces the preparation efficiency of ultrafine-grained copper alloys [59]. The mechanism is a continuous stacking and rolling process of plate materials (see Figure 1c). In this process, the original plate is placed on the other plate orderly, and the plate is rolled and welded together through the traditional rolling and welding process. When necessary, the surface treatment between the stacking layers is carried out to improve its bonding strength. Then, the intermediate plate is cut into two parts, and the two parts are surface treated and stacked, and then the cyclic rolling and welding is carried out. The whole process needs to be carried out at high temperature below the recrystallization temperature. If the temperature is too high, the recrystallization of the material occurs, which offsets the cumulative strain generated in the rolling process. In contrast, at lower temperature the ductility and bond strength decrease.

In conclusion, SPD is an effective method to prepare ultrafine or even nanocrystalline copper alloys, which greatly improves the properties in traditional ways. Compared to undeformed or small deformed coarse-grained ones, the copper alloys prepared by SPD have a higher strength due to the ultrafine grain and high defect density. However, such microstructure characteristics also significantly reduce the ductility. For instance, Segal [60] studied the relationship between the strength, elongation, and extrusion passes of Armco steel after ECAP process. It was found that the tensile strength increased with the increase of extrusion passes. The tensile strength increased from 300 MPa to 750 MPa after one pass extrusion, and the tensile strength increased during the subsequent eight passes extrusion. However, the ductility decreased significantly from 20% to several percent, after eight passes extrusion. The sharp drop in ductility is due to the inability of dislocations to produce and move in ultrafine grains during plastic deformation [61].

In addition, the size of workpieces that can be processed by SPD methods is often small, and high-power equipment and expensive dies are demanded, which thereby makes it difficult to be widely used in industrial production. Some SPD methods have the problem of fatigue cracks during workpiece deformation, such as ARB.

2.3. Summary and Outlook

According to the above discussion in this section, traditional strengthening methods of copper alloys, including second phase dispersion strengthening and ultrafine grain strengthening, have been extensively studied. But both have drawbacks in their respective strengthening methods and preparation processes. In addition, the most critical contradiction between strength and plasticity of copper alloy has not been effectively solved. The shackles of these conventional ideas and methods demand to be broken, and the advantages of dispersion strengthening and grain-refining strengthening are better when combined through simple processes (e.g., the casting process), preparing copper alloy with both high strength and high ductility, which is supposed to greatly improve the current situation of strengthening and toughening in copper alloys.

3. In-Situ Nano Precipitate Reinforced Copper and Copper Alloys

3.1. Design Idea and In-Situ Fabrication Route

Nanoparticle precipitation strengthening has been widely used in the strengthening of metallic materials. The literature shows that the coordination of strength and ductility is achieved by using nano precipitate strengthening. By tailoring the precipitation process of Ni (Al, Fe) phase, Z. P. Lu et al. [62] prepared highly dispersed and fully coherent nano-sized Ni (Al, Fe) particles in the steel, which broke the strength-ductility inversion and strengthened the alloy without sacrificing ductility. The strength reached 2.2 GPa and the plasticity remained at about 8.2%. C.T. Liu et al. [63] achieved the balance of strength and ductility by controlling the precipitation of Ti-Al intermetallic nanoparticles in (FeCoNi)₈₆-Al₇Ti₇ (Al₇Ti₇) alloy matrix. The tensile fracture strength at room temperature exceeded 1500 MPa, and the elongation was still as high as 50%. It is believed that the

coherent or semi-coherent interface between the nano precipitate and the matrix is an obstacle to hinder and store dislocations, and to become a sustainable source of dislocation nucleation. This interface provides more space to accommodate dislocations, and produces the synergistic effect of strengthening and plasticizing for metal materials [64].

The solubility of Fe and Co in copper is high at elevated temperature, but at room temperature the solubility of Fe and Co in copper is very low and almost insoluble in copper matrix [44,65,66]. This characteristic is the premise of in-situ nano iron-rich precipitate strengthening in copper. The dispersion particle reinforced copper matrix composites, prepared by external addition reinforced particles or precipitation of reinforced particles in the aging process, present some problems in technology and performance. The main problem is that the reinforced particles not only improve the strength, but also damages the elongation of the alloy. The larger the particle size is, the greater the damage is, and the reinforced particle cannot improve the microstructure of the alloy.

Wang et al. [29,31,32,43–46] proposed a new idea to prepare copper alloy by preparing nano precipitate in-situ formed in the casting process (including solidification of metal melt and cooling of solid matrix), and obtained NPF structure in copper alloy. During the casting process of copper alloy, the raw materials doped with iron, cobalt, copper, and other alloying elements, are added into the graphite crucible, and the crucible is heated to about 1300 °C and maintained for 20–30 min under electromagnetic induction. The electromagnetic induction heating process causes strong convection in the copper melt, and the density of iron, cobalt, and copper atoms, is very close at 7.8×10^3 , 8.9×10^3 , and $8.9 \times 10^3 \text{ kg}\cdot\text{m}^{-3}$, respectively. Consequently, these atoms are uniformly distributed in the melt under the intense convection (stage I in Figure 2). The uniform distribution of iron and cobalt elements in the melt promotes the subsequent uniform precipitation of iron-rich nanoparticles in the melt and copper matrix. After the melt is poured into the graphite mold, the temperature decreased and the iron-rich nanoparticles uniformly precipitated in the melt. Due to the iron-rich nanoparticles having a good crystallographic match with the copper matrix, sufficient size, and quantity density, efficient heterogeneous nucleation of copper melt occurs with iron-rich nanoparticles as the substrate at a certain undercooling (stage II in Figure 2). This heterogeneous nucleation effect from iron-rich nanoparticles effectively refines the copper grains [44,48]. In addition, during the nucleation and growth of copper crystals, most of the iron-rich nanoparticles fail to become the substrate for heterogeneous nucleation, and are spontaneously captured by the liquid-solid interface during the growth of copper grains/crystals (stage II in Figure 2) and dispersed inside the copper grains [67]. After solidification, during the cooling process of solid copper alloy, the new iron-rich nanoparticles nucleate and grow in the solid matrix, along with the evolution of crystal structure and morphological transition from spherical to petal-like shape [44,47]. In addition, some iron-rich nanoparticles pin grain boundaries and hinder grain growth (stage III in Figure 2). Finally, most of the iron-rich nanoparticles are uniformly dispersed within the refined micron-sized copper matrix grains to form the NPF structure.

Overall, the dispersion precipitation strengthening alloy has made great progress. For copper alloy, one way is to add carbides (SiC, TiC), borides (TiB₂), and nitrides, by means of external addition such as mechanical alloying and powder metallurgy to obtain dispersion strengthened copper alloy. However, the dispersion phase obtained by this method is often difficult to uniformly distribute in the matrix, and the dispersion particles are susceptible to pollution and have a bad matching relationship with the matrix. There are also cost problems and product size constraints.

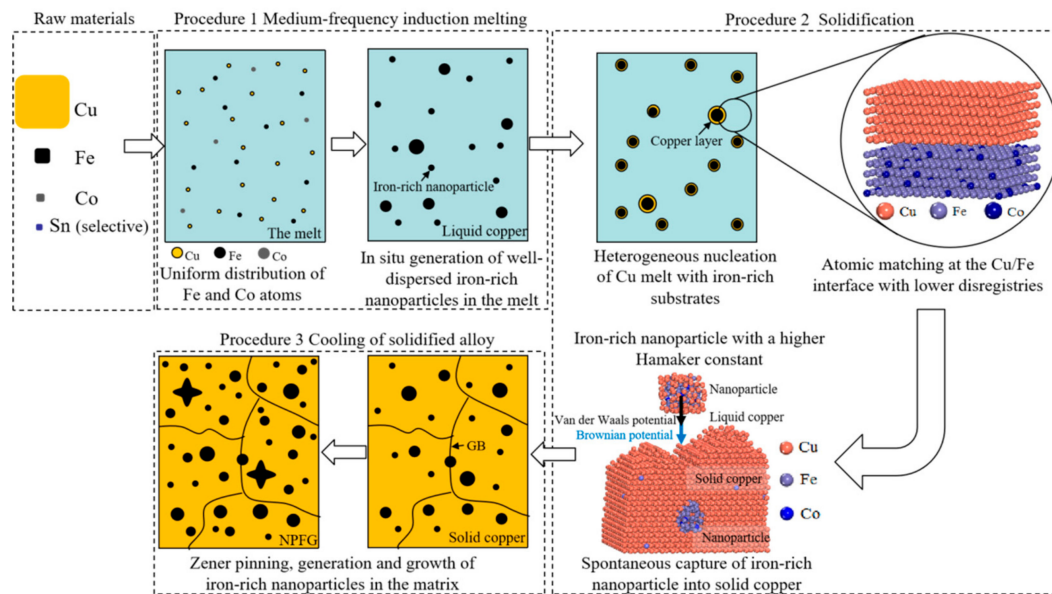


Figure 2. Schematic of microstructural evolution during casting process that produced NPFGB structure [44].

The second method is to obtain dispersed copper alloy by in-situ precipitation, which has the following advantages compared with the external method: (1) The addition of microalloying elements (such as Fe, Co) as heterogeneous nucleation core. In the solidification process, the in-situ nucleation of precipitates occurs in the melt, and further reduces the nucleation energy of copper matrix melt, and thence refine the copper grains, which improve the strength of the alloy. (2) In-situ nanoparticle strengthening. Compared with the traditional micron and submicron particles, the in-situ generated nano-scale dispersion particles have a good interface relationship with the matrix, which is coherent and semi-coherent. The in-situ nanoparticles with high number density have more obvious dislocation obstruction in copper alloys, and the ability to accommodate dislocations at the particle/matrix interface is stronger, which effectively alleviates dislocation accumulation and stress concentration. Therefore, while improving the strength of the material, the ductility damage of the material is also reduced to the minimum. However, the research on in-situ nanoparticles reinforced copper alloy technology is still relatively limited, and there is a long way to go from laboratory to industrial production.

3.2. Microstructural and Mechanical Characteristics

3.2.1. NPFGB Structured tin Bronze Alloy

Wang et al. [29,31,32,43–46] proposed the concept of in-situ nano precipitate-fine grain (NPFGB) structure prepared by casting process, in view of the disadvantages of the traditional second phase dispersion strengthening and ultrafine-grain strengthening in their respective strengthening methods and preparation processes. The NPFGB strategy has been applied in tin bronze alloys.

During the solidification process, the matrix grains of copper alloy are refined to 1–100 μm induced by in-situ precipitation of iron-rich nanoparticles in high-temperature copper melt. Specifically, the solidification microstructure of as-cast Cu-10Sn-2Zn-1.5Fe-0.5Co alloy is significantly refined, and the average size of equiaxed grains is reduced to 23 μm (Figure 3b). In contrast, as-cast Cu-10Sn-2Zn alloy shows a typical dendritic structure, and the size of the primary dendrite arm is about 200 μm (Figure 3a). In addition, Sn-rich δ phases are continuously distributed between the dendrite arms [48]. In the as-cast Cu-10Sn-2Zn-1.5Fe-0.5Co alloy, the iron-rich nanoparticles are dispersed in the refined grains, forming the NPFGB structure. The formation of NPFGB structure has a significant

effect on preventing Sn segregation, and thus the formation of Sn-rich δ phases at grain boundaries in tin bronze alloy (see Figure 4).

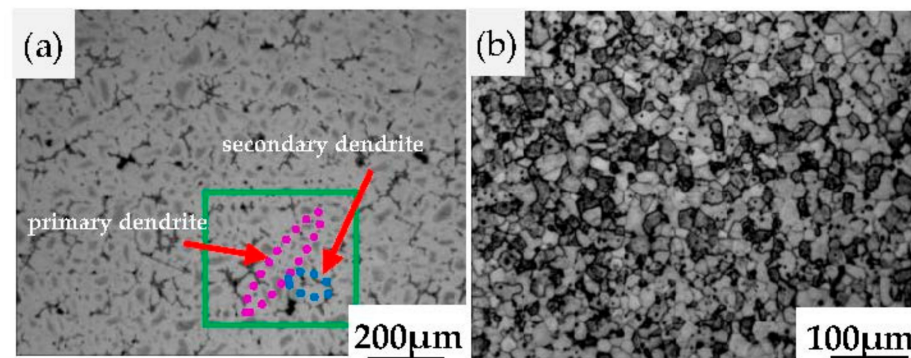


Figure 3. Optical micrographs (OM) of the samples showing the effect of Fe, Co on grain refinement. (a) OM of Cu-10Sn-2Zn alloy; (b) OM of Cu-10Sn-2Zn-1.5Fe-0.5Co alloy [48].

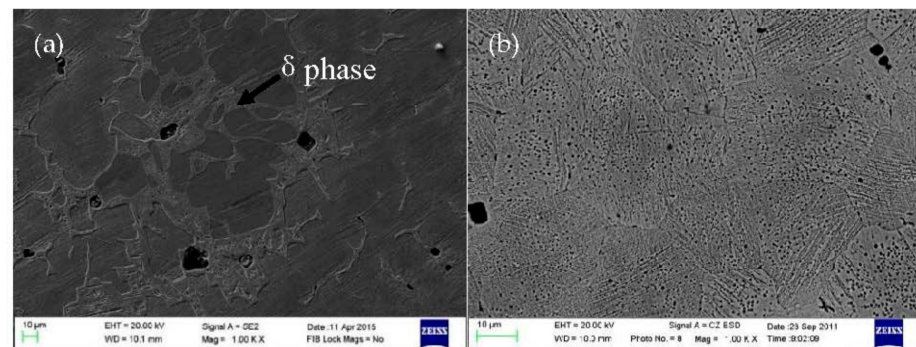


Figure 4. SEM micrographs showing microstructure of the samples: (a) Etched Cu-10Sn-2Zn alloy sample; (b) Etched Cu-10Sn-2Zn-1.5Fe-0.5Co alloy sample [68].

As seen in Figure 4a, tin-rich δ phase in the as-cast Cu-10Sn-2Zn alloy is frequently distributed between dendrites and is almost completely connected. However, in the as-cast Cu-10Sn-2Zn-1.5Fe-0.5Co alloy, most regions are non-tin-rich phase regions (Figure 4b) [68]. The iron-rich nanoparticles are in the form of face-centered cubic (f.c.c.) and body-centered cubic (b.c.c.) structures (Figure 5). The f.c.c. iron-rich nanoparticles satisfy a cube-on-cube orientation and maintain a coherent relationship with the copper matrix (Figure 5a–c). For iron-rich nanoparticles with b.c.c. structure, K-S orientation (i.e., $(110)[111]_{\alpha\text{-Fe}} // (111)[111]_{\text{Cu}}$) and semi-coherent interface is maintained with the matrix (Figure 5d–f) [42]. The strength and ductility of as-cast Cu-10Sn-2Zn-1.5Fe-0.5Co alloy are improved simultaneously due to the formation of NPF structure and the elimination of serious segregation [29,31,48]. The ultimate tensile strength, yield strength, and total elongation of as-cast Cu-10Sn-2Zn-1.5Fe-0.5Co alloy are increased from 225 MPa, 128 MPa and 12 % to 463 MPa, 215 MPa and 28 %, respectively (Figure 6) [48].

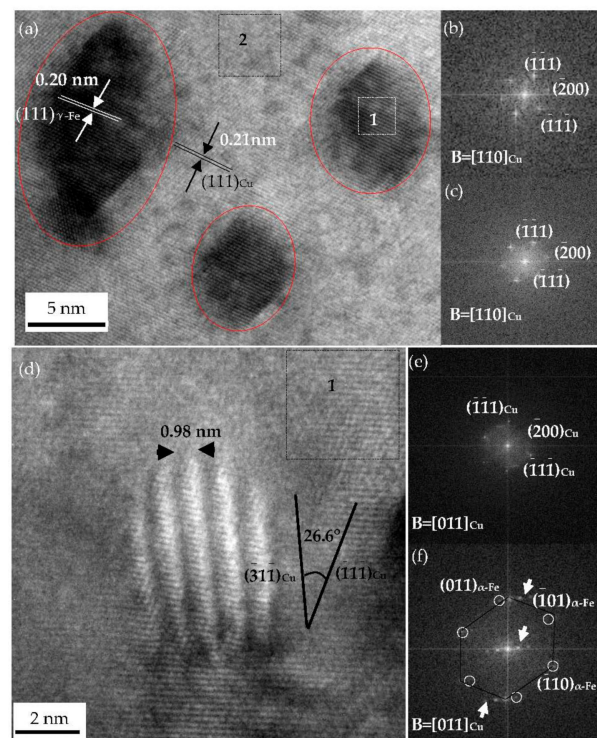


Figure 5. HRTEM and Cs-corrected STEM micrographs of γ -Fe nanoparticles in as-cast Cu-10Sn-2Zn-1.5Fe-0.5Co alloy and their FFT patterns: (a) HRTEM micrograph of iron-rich nanoparticles when the incident electron beam is parallel to $\langle 110 \rangle_{\text{Cu}}$; (b,c) FFT patterns of position 1 and 2 in (a), respectively; (d) HRTEM image of a single iron-rich nanoparticle taken from the specimen. Zone axis: $[011]_{\text{Cu}}$; (e) Diffractogram taken from position 1 in (d); (f) Diffractogram taken from the HRTEM image of (d), where FFT pattern of Cu matrix and iron-rich nanoparticle are indicated by black lines and white circles, respectively [42].

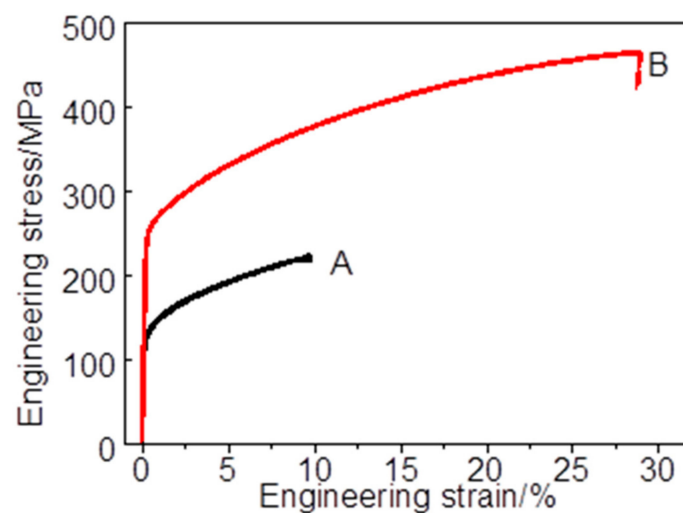


Figure 6. Curves A and B are tensile engineering stress–strain curves of as-cast Cu-10Sn-2Zn and Cu-10Sn-2Zn-1.5Fe-0.5Co alloys, respectively [48].

Chen et al. [69] studied as-cast Cu-12Sn-1.5Ni bronze alloys with different iron contents (0, 0.053, 0.63 and 1.44 wt.% Fe). The individual addition of iron also induces the formation of NPF structure and the elimination of coarse segregation phase. In the original Cu-12Sn-1.5Ni, the dendrites of α -Cu phase are very coarse (Figure 7a,b), while the grains of Cu-12Sn-1.5Ni- x Fe alloys with different iron contents have refined (Figure 7c–h). When

For $\text{Fe} \leq 0.5 \text{ wt.}\%$, the grain size decreases significantly with the increase of Fe content, but the degree of grain refinement tends to be flat when $\text{Fe} > 0.5 \text{ wt.}\%$ (Figure 7i). The grain refinement is mainly related to two factors of heterogeneous nucleation and recalcification during crystal growth [70–73].

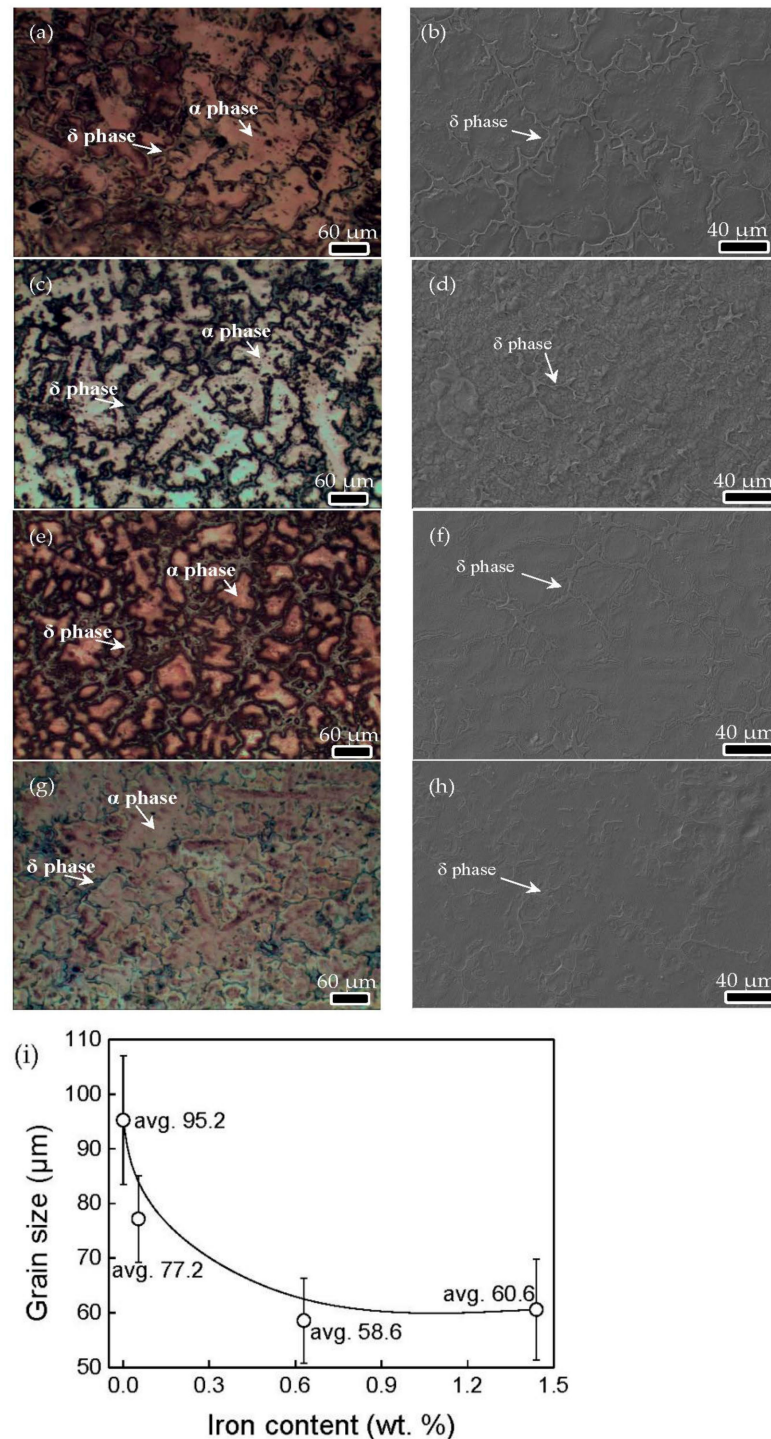


Figure 7. (a,c,e,g) OM and (b,d,f,h) SEM micrographs of cast (a,b) Cu-12Sn-1.5Ni; (c,d) Cu-12Sn-1.5Ni-0.05Fe; (e,f) Cu-12Sn-1.5Ni-0.5Fe; (g,h) Cu-12Sn-1.5Ni-1.5Fe alloys. Dendritic or grain matrix of α phase and interdendritic δ phase were indicated by white arrows and labels; (i) Grain size as a function of iron content in cast Cu-12Sn-1.5Ni-xFe alloys [69].

During solidification of Cu-12Sn-1.5Ni-(0.05~1.5)Fe alloys, iron-rich nanoparticles precipitate in the copper melt in advance, which provides heterogeneous nucleation cores for copper melt and produces grain refinement [48,49]. In the meantime, latent heat is released during crystal growth of copper, resulting in the decrease of cooling rate and the increase of melt temperature around the crystal (i.e., recalescence). This recalescence effect hinders the undercooling required for heterogeneous nucleation of copper melt on other iron-rich nanoparticles, which results in the suppression of further grain refinement when the iron content is higher than 0.5 wt.%. In terms of tin segregation, compared with the original Cu-12Sn-1.5Ni alloy, the distribution of the δ phase in the Cu-12Sn-1.5Ni-(0.05~1.5) Fe alloy at the grain boundary is more dispersed and the size is smaller (Figure 7d,f,h).

The precipitation features of Cu-12Sn-1.5Ni alloy with different iron contents (0, 0.053, 0.63, 1.44wt.%) are also different. In Cu-12Sn-1.5Ni-0.05Fe alloy, a large number of dot-like nano-sized particles dispersed in the copper matrix (Figure 8b); in Cu-12Sn-1.5Ni-0.5Fe, in addition to dispersed dot-like nanoparticles, larger spherical nanoparticles appear in the matrix (Figure 8c); in Cu-12Sn-1.5Ni-1.5Fe alloy, large cubic particles are distributed in the matrix simultaneously with spherical and dot-like nanoparticles (Figure 8d). Studies have shown that the dot-like nanoparticles are iron-rich phase with f.c.c. structure [42,44,48], and the cuboidal and spherical ones are with b.c.c. structure [42,44,47,48]. With the increase of iron content, the morphology of iron-rich precipitates changes from dot-like to spherical, to cuboidal during coarsening, which is consistent with the morphology evolution path of iron-rich phase in pure copper [47]. Therefore, the individual addition of iron leads to the decrease of grain size of as-cast Cu-12Sn-1.5Ni alloy, the formation and uniform distribution of iron-rich nanoparticles in the copper matrix, and the elimination of coarse continuous brittle δ phase between dendrites. This microstructural optimization leads to the simultaneous increase in strength and plasticity of as-cast Cu-12Sn-1.5Ni-(0.05~1.5)Fe alloys, in comparison with the original Cu-12Sn-1.5Ni alloy (Figure 9). In particular, when the iron content reaches 1.44 wt.%, the tensile strength of the alloy increases from 327.36 MPa in the original state to 440.99 MPa. When the iron content was 0.053 wt.%, the uniform elongation and elongation after fracture increased significantly, reaching the impressive values of $20.44 \pm 3.80\%$ and $21.43 \pm 3.89\%$, respectively.

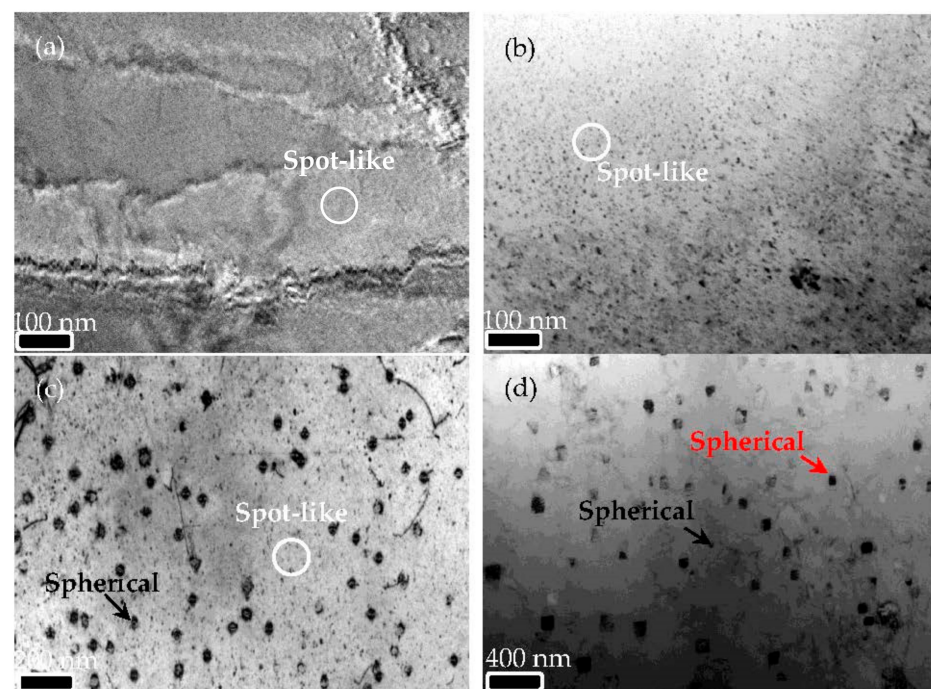


Figure 8. Bright-field TEM images showing the precipitates in (a) Cu-12Sn-1.5Ni; (b) Cu-12Sn-1.5Ni-0.05Fe; (c) Cu-12Sn-1.5Ni-0.5Fe; (d) Cu-12Sn-1.5Ni-1.5Fe alloys [69].

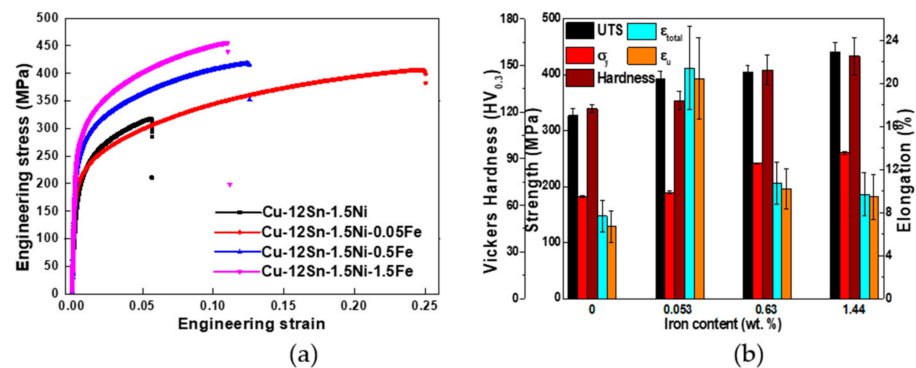


Figure 9. (a) Engineering stress vs. strain curves; (b) Tensile properties and hardness (HV0.3) [69].

In general, the formation of NPF structure induced by in-situ formation of nanoparticles by introducing trace Fe and Co elements into copper alloy optimizes microstructure and greatly improves the mechanical properties of tin bronze alloy. First, copper matrix grain refinement. Second, the inhibition of tin segregation (hindering the formation of brittle tin-rich phase at grain boundaries). Third, improvement in the strength and plasticity at the same time. In addition, it should be noted that the addition Fe and Co elements on the microstructural optimization and mechanical improvement is limited, which is closely related to the addition amount of microalloying elements. The variation of Fe and Co additions directly affects the size, number density, crystal structure, and interface feature, of the iron-rich nanoparticles, thereby affecting the mechanical properties. The heterogeneous nucleation mechanism of iron-rich nanoparticles, the capture mechanism of nanoparticles by solidification front, the inhibition mechanism of tin segregation, and the strengthening and plasticizing mechanism of the alloy, will be discussed and explained in the following Sections 3.2–3.4.

3.2.2. NPF Structured Copper

In addition to NPF structured tin bronze alloy with improved comprehensive mechanical properties, Chen et al. [44,46] introduced NPF structure into pure copper by adding iron, cobalt, and minor tin in the casting process.

The results show that pure copper exhibits uneven grain size (see the error bar in Figure 10g) and morphology (Figure 10a), as well as uneven shrinkage size (the size fluctuation of different parts is about 1~60 μm , as shown in Figure 10a). After adding iron and cobalt, the matrix grains of Cu-Fe-Co alloy undergo typical columnar-to-equiaxed transition (CET), and the equiaxed grain size decreases with the increase of iron content (Figure 10a–e,g). The grain size of Cu-Fe-Co alloy with a certain iron content is significantly larger than that of tin bronze alloy with the same iron content (see Figure 7). The two types of alloys have similar grain refinement trends, that is, when the iron content is low ($\leq 1.5\text{wt.}\%$), the average grain size decreases greatly with the increase of iron content. However, the grain refinement effect decreases significantly with the increase of iron content above 1.5 wt.%. This phenomenon is also present in the bronze alloy, and for instance the grain size levels off in Cu-12Sn-1.5Ni alloy when the iron content exceeds 0.5 wt.% (Figure 7).

This grain refining trend can be explained from two aspects. Firstly, when the iron content is low, the number density and size distribution width of iron-rich nanoparticles are insufficient, and the refinement effect is limited. With the increase of iron content, the number density and size distribution width of iron-rich nanoparticles increase accordingly, which serve as nucleation cores with high potential to significantly refine the matrix grains. On the other hand, the growth of the nucleation crystals releases latent heat and produces recalescence, which prevents other iron-rich nanoparticles from obtaining the undercooling required for copper nucleation [71,72]. Therefore, the grain refinement effect is not infinitely enhanced with the increase of iron content.

The recalescence caused by crystal growth can be weakened by the growth restriction effect, that is, the solute elements discharged to the liquid-solid interface hinders the continuous growth of the crystal and weakens the release of latent heat [74,75]. In this context, more heterogeneous nucleation cores are capable of reaching the critical undercooling required for nucleation, and thence to promote more excellent grain refinement. This explains why the grain size of Cu-Fe-Co alloy with a certain iron content is significantly larger than that of tin bronze alloy with the same iron content. That is to say, Sn and Zn in tin bronze alloy inhibit the growth of copper crystal, and promote more iron-rich nanoparticles to play the role of heterogeneous nucleation, resulting in a greater refinement effect than that of Cu-Fe-Co alloy.

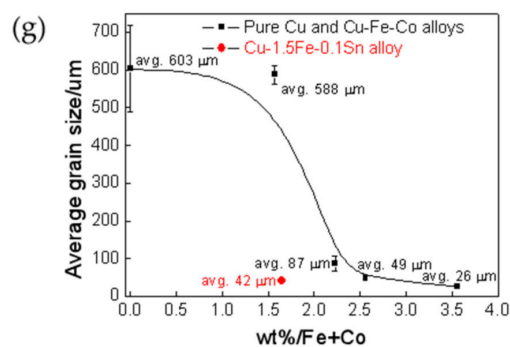
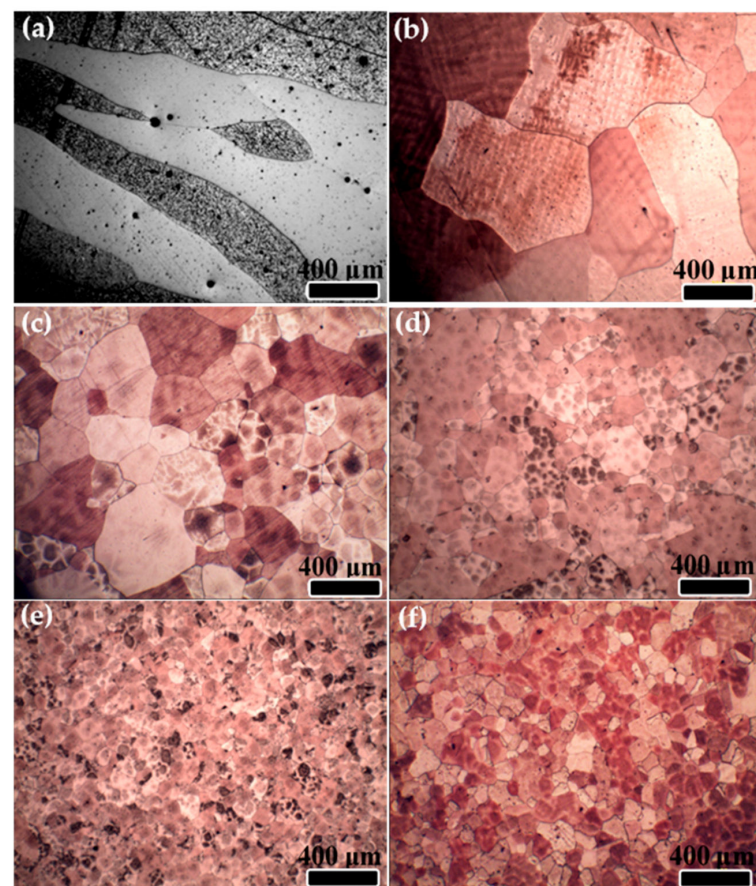


Figure 10. Optical micrographs (OM) of as-cast samples showing the effect of Fe+Co content and minor solute Sn on grain refinement. (a) Pure Cu; (b) Cu-1.0Fe-0.5Co alloy; (c) Cu-1.5Fe-0.5Co alloy; (d) Cu-2.0Fe-0.5Co alloy; (e) Cu-3.0Fe-0.5Co alloy; (f) Cu-1.5Fe-0.1Sn alloy; (g) Grain size (with standard deviation bars) as a function of actual Fe+Co content [44].

According to the strong growth restriction of tin, Chen et al. [44] co-introduced iron and tin elements into pure copper to prepare as-cast Cu-1.5Fe-0.1Sn alloy. The grain size was refined into about 42 μm in Cu-1.5Fe-0.1Sn alloy (Figure 10 f,g), smaller than that of Cu-2.0Fe-0.5Co alloy, although the Fe + Co content of the former is lower than that of the latter. These results show that the addition of minor Sn improves the efficiency of grain refinement of iron and/or cobalt. As a whole, in order to prepare as-cast alloys with NPGF structure, not only the nano precipitates with high potential and high number density are required, but also the appropriate solute elements are needed to play the role of growth restriction.

The addition of Fe and Co during casting of pure copper induces the formation and evolution of iron-rich nanoparticles in copper matrix [44,46,47]. In Cu-(1.0, 1.5)Fe-0.5Co alloy, dot-like and spherical particles with high number density are dispersed in the copper matrix (see Figure 11a,b). With the increase of iron content, large-sized petal-like particles appear in Cu-(2.0,3.0)Fe-0.5Co alloy, along with a large number of dot-like and spherical particles (Figure 11c,d). The branches of petal-like iron-rich particles inside the same grain grow symmetrically along the identical orientation of the matrix. Petal-like shape was not found in Cu-(1.0,1.5) Fe-0.5Co alloy, indicating that iron content strongly affected particle morphology.

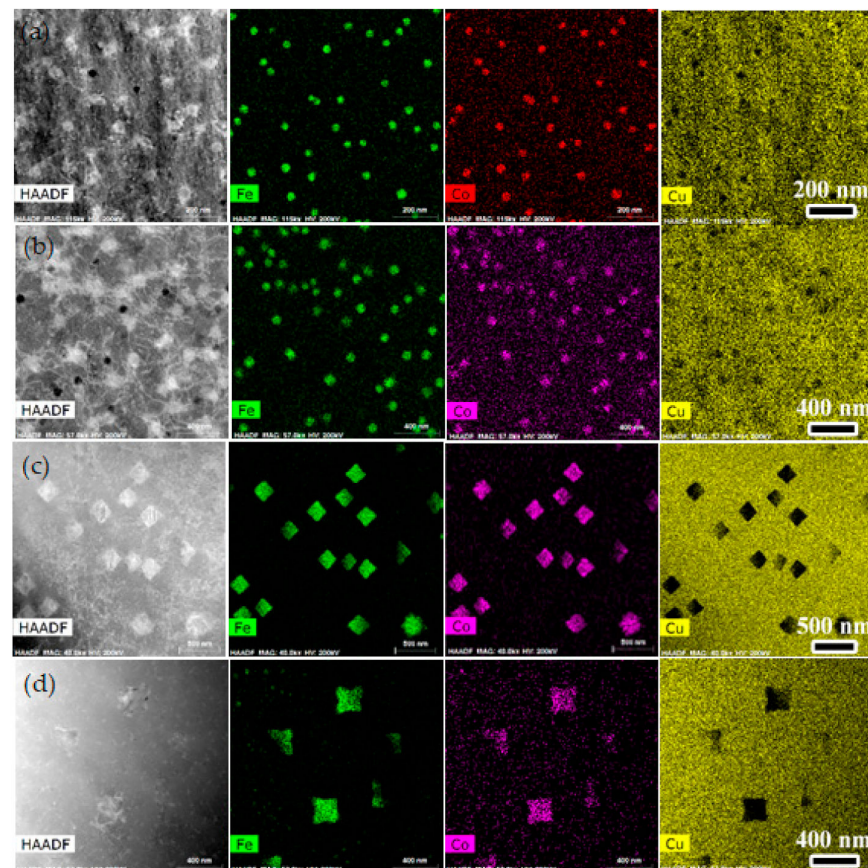


Figure 11. HAADF or BF images of iron-rich nanoparticles and their corresponding elemental maps. (a) Spherical nanoparticles in Cu-1.0Fe-0.5Co alloy; (b) Spherical nanoparticles in Cu-1.5Fe-0.5Co alloy; (c) Petal-like nanoparticles in Cu-2.0Fe-0.5Co alloy; (d) Petal-like nanoparticles in Cu-3.0Fe-0.5Co alloy.

In addition to the morphological evolution, with the increase of iron content, the size and number density of the particles increase and decrease respectively, and the size distribution width of nanoparticles also increases with the increase of iron content. There are many types of iron-rich nanoparticles in this kind of alloy, including f.c.c. dot-like nanoparticles

(<20 nm) with cube-on-cube orientation, b.c.c. spherical nanoparticles (20~150 nm) with K-S orientation, and b.c.c. petal-like nanoparticles (100~600 nm) with K-S orientation [44,47].

The strength and ductility of NPFG-structured Cu-Fe-Co and Cu-1.5Fe-0.1Sn alloys increase simultaneously, almost twice as much as that of coarse-grained pure copper (Figure 12a,b) [46]. For Cu-1.0Fe-0.5Co alloy, the addition of Fe and Co increases the tensile strength σ_{UTS} from 152 MPa to 267 MPa, and the yield strength σ_s from 58 MPa to 118 MPa (Figure 12a), respectively. Meanwhile, the total elongation δ_f and uniform elongation δ_u increase slightly (Figure 12b). With the increase of Fe content in Cu-Fe-Co alloy, the yield strength σ_s first increases (when Fe \leq 1.5 wt.%) and then decreases slightly (when Fe > 1.5wt.%), as shown in Figure 12a. This variation of yield strength is related to grain refinement and the evolution of iron-rich nanoparticles. The strengthening mechanism will be discussed in Section 3.3. Different from the yield strength, the tensile strength σ_{UTS} and elongation (δ_f and δ_u) increase with the increase of iron content (Figure 12a,b). The improvement of σ_{UTS} and δ_u is related to strain hardening rate Θ , and the value of Θ strongly depends on the grain size [76]. Compared with pure copper, Cu-1.0Fe-0.5Co alloy exhibits obvious work hardening (Figure 12c,d), which is attributed to the high-level dislocation storage efficiency generated by the interaction of iron-rich nanoparticles and dislocations.

Qin et al. [77] studied the strengthening effect of SiC particles on 6061 aluminum matrix composites by using the finite element method (FEM). The results indicated that the residual stress and strain concentration occur near the particles with sharp corners during plastic deformation, and the concentration of stress and strain induce the initiation of micro cracks under small external stress, thus reducing the plasticity of the material. The morphological effect of this strengthening particle on the ductility is also exhibited in the γ -Al₂O₃ nanoparticles reinforced copper alloy [78].

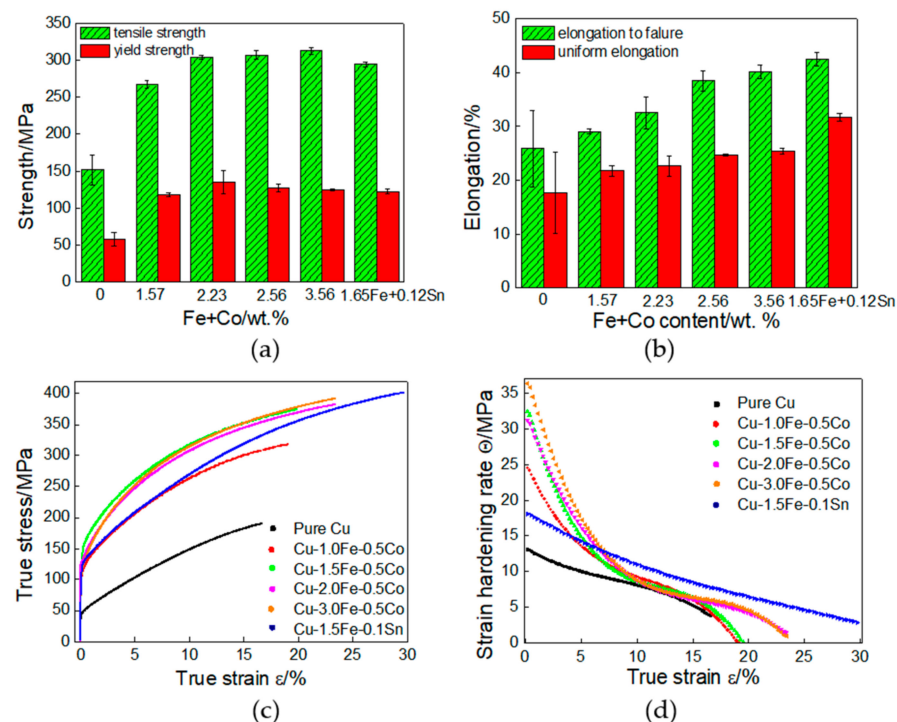


Figure 12. Comparison of room-temperature tensile behavior for the samples. (a) Ultimate tensile stress σ_{UTS} , yield tensile stress σ_s ; and (b) Elongation to failure δ_f and uniform elongation δ_u of the as-cast samples (with standard deviation bars). All states were tested in quadruplicate and the error bars plotted in (a,b) represent the full range of scatter amongst the four tests for each state examined; (c) Tensile true stress-strain curves converted from the engineering stress-strain curves by using Standard textbook equations; (d) Strain-hardening curves. Strain-hardening rate $\Theta = d\sigma/d\varepsilon$, where σ and ε are true stress and true strain, respectively [46].

With regard to iron-rich nanoparticles in NPFG structured copper alloys, the spherical morphology of interface passivation instead of the petal-like and cubic morphology with sharp corners is bound to reduce the residual stress and strain concentration near the iron-rich nanoparticles, thereby improving the deformation behavior and deformation plasticity of the alloy. In terms of particle size, the crack tends to initiate at the interface of large particles due to the low interfacial adhesion of large particles. The interface between the smaller nanoparticles and the matrix is more coherent, so it is necessary to produce the interface cracking under higher strain conditions, which is beneficial to the ductility improvement of the alloy [76,79]. When the iron content is high (e.g., Cu-(2.0,3.0)Fe-0.5Co alloys), the iron-rich nanoparticles are obviously coarsened, and a large number of coarsened particles show petal-like morphology. The existence of these particles leads to the generation and coalescence of micropores under low strain, thereby causing the decrease of uniform elongation and total elongation of the alloy.

Overall, compared with the more complex tin bronze alloy system, the introduction of trace Fe and Co, Sn elements in pure copper can also refine the copper matrix and disperse the iron-rich nanoparticles, forming NPFG structure to strengthen the alloy. It is worth noting that, similar to the tin bronze alloy, the introduction of iron-rich nanoparticles in pure copper has an upper limit relative to the refinement of the matrix, and the grain refinement effect will be significantly weakened when the value exceeds this limit (Figures 7I and 10g). This phenomenon also exists in the tin bronze alloy system, which proves that the grain refinement effect is not infinitely enhanced with the increasing content of micro-alloy elements.

In addition, further studies on the nano-sized iron-rich nanoparticles in pure copper system also show that the iron content makes the morphology of the nanoparticles evolve (Figure 11), and also strongly affects the size distribution, quantitative density, and crystal structure of nanoparticles. When the iron content is too high, it will change from spherical to cuboidal, and even to petal-like, and produce sharp corners along specific orientations, which have a negative impact on the mechanical properties, in particular to ductility, of the alloy. In fact, in the subsequent Sections 3.3 and 3.4, the yield strength increment calculation also proves that the size of nanoparticles will affect the strengthening mechanism. Therefore, for different copper alloy systems, the addition ratio of iron content must be reasonably set in the construction of NPFG structure, so as to improve the microstructure and mechanical behavior of NPFG-Cu. However, in general, the formation of this NPFG structure also improves the strength and plasticity of pure copper system.

3.3. Mechanism of Strengthening and Plasticizing

The synchronous improvement of strength and ductility of NPFG-structured copper alloy mainly comes from its refined grains and iron-rich nanoparticles dispersed within grains [46]. The yield strength is the superposition of precipitation strengthening from iron-rich nanoparticles, grain-refining strengthening and solid-solution strengthening from Fe, Co, Sn atoms dissolved in the matrix [80,81]. For precipitation strengthening, several kinds of iron-rich nanoparticles exist in NPFG copper alloy with dot-like, spherical, cubic, and petal-like shapes. The influence of nanoparticles with various sizes and shapes on mechanical properties is more complex than that of a single type of precipitate strengthening. Studies have shown that the overall strengthening effect of multiple particles is the linear superposition of various precipitate strengthening effects, and the superposition process includes two ways, i.e., whether the relative density of various particles is considered [82,83].

The spherical, cuboidal, and petal-like nanoparticles in NPFG-structured copper alloys are centrally symmetrical, and the composition of the particles is similar. The size, number density, and volume fraction of the particles can be quantitatively characterized. Therefore, Chen et al. [46] unified the strengthening effect of spherical, cuboidal, and petal-like iron-rich nanoparticles with spherical precipitation strengthening model. Two typical precipitation strengthening models are attempted to calculate the strengthening

effect of iron-rich nanoparticles ($\Delta\sigma_{\text{nanoparticle}}$), which is the shearing mechanism [80–84] and the Orowan-looping mechanism [82,83,85]. In the former, the strengthening effect of deformable particles on the dislocation slip includes chemical strengthening ($\Delta\sigma_{\text{Chemical}}$), modulus strengthening ($\Delta\sigma_{\text{Modulus}}$), coherent strengthening ($\Delta\sigma_{\text{Coherency}}$), and ordered strengthening ($\Delta\sigma_{\text{Order}}$). The contribution of deformable particles to the increment of yield strength ($\Delta\sigma_s$) can be expressed by the following formula (only $\Delta\sigma_{\text{Chemical}}$, $\Delta\sigma_{\text{Modulus}}$ and $\Delta\sigma_{\text{Coherency}}$ are considered) [82]:

$$\Delta\sigma_{\text{Chemical}} = 0.8M \cdot 2 \left(\frac{3}{\pi} \right)^{\frac{1}{2}} \mu_{\text{matrix}} \left(\frac{\gamma}{\mu_{\text{matrix}} b} \right)^{\frac{3}{2}} \left(\frac{b}{r} \right) f^{1/2} \quad (1)$$

$$\Delta\sigma_{\text{Modulus}} = 0.8M \cdot 0.9 (rf)^{\frac{1}{2}} \left(\frac{1}{2} \mu_{\text{matrix}} b \right) \left(\frac{\Delta\mu}{\mu_{\text{matrix}}} \right)^{\frac{3}{2}} \left[2b \ln \left(\frac{2r}{f^{\frac{1}{2}} b} \right) \right]^{-\frac{3}{2}} \quad (2)$$

$$\Delta\sigma_{\text{Coherency}} = 0.8Mk^{3/2} \mu_{\text{matrix}} \varepsilon^{3/2} \left(\frac{r}{b} \right)^{\frac{1}{2}} \left(\frac{3}{2\pi} \right)^{\frac{1}{2}} f^{1/2} \quad (3)$$

The contribution of the strengthening effect by Orowan-looping mechanism to the $\Delta\sigma_s$ is:

$$\Delta\sigma_{\text{Orowan}} = 0.8M \left(\frac{3}{2\pi} \right)^{1/2} \frac{\mu_{\text{matrix}} b}{r} f^{1/2} \quad (4)$$

By comparing the predicted precipitation strengthening value $\Delta\sigma_{\text{nanoparticle}}$ obtained by the above model with the experimental value $\Delta\sigma_s$ (exp.) of the actual yield strength increment, it is found that the predicted value $\Delta\sigma_{\text{Orowan}}$ by the Orowan mechanism is very close to $\Delta\sigma_s$ (exp.), while the predicted values of shearing mechanism $\Delta\sigma_{\text{Chemical}}$, $\Delta\sigma_{\text{Modulus}}$, and $\Delta\sigma_{\text{Coherency}}$ are much larger or far smaller than $\Delta\sigma_s$ (exp.) (Figure 13a), which proves that the description of the Orowan-looping model satisfies the strengthening effect of iron-rich nanoparticles in the NPFG structure copper alloy.

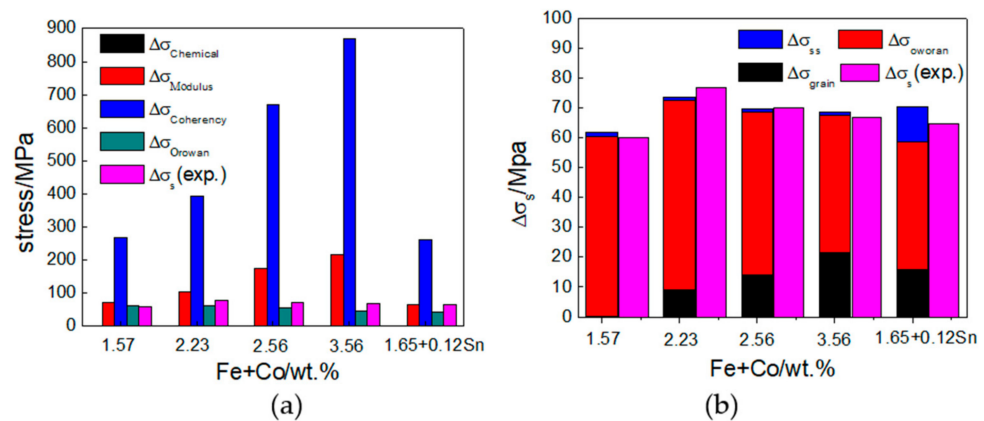


Figure 13. (a) Experimental values of overall yield strength increment $\Delta\sigma_s$ (exp.) (purple bar) and predicted precipitation strengthening $\Delta\sigma_{\text{nanoparticle}}$ arising from spherical and petal-like nanoparticles as a function of $\Delta\sigma_{\text{Chemical}}$ (black bar), $\Delta\sigma_{\text{Modulus}}$ (red bar), $\Delta\sigma_{\text{Coherency}}$ (blue bar), and $\Delta\sigma_{\text{Orowan}}$ (green bar); (b) Predicted values of overall yield strength increment $\Delta\sigma_s$ containing grain-refined strengthening $\Delta\sigma_{\text{grain}}$ (black bar), solid-solution strengthening $\Delta\sigma_{\text{ss}}$ (blue bar), and precipitation strengthening $\Delta\sigma_{\text{Orowan}}$ (red bar), compared with experimental values of overall yield strength increment $\Delta\sigma_s$ (exp.) (purple bar). The modeling predictions agree with the measured behaviors although it is shown that some refinements to the description of strengthening models are required [46].

For fine grain strengthening, $\Delta\sigma_{\text{grain}}$ can be calculated by Hall-Petch relation [2,3], and the calculation formula is:

$$\Delta\sigma_{\text{grain}} = k \left(d_2^{-1/2} - d_1^{-1/2} \right) \quad (5)$$

The d_1 and d_2 are the average grain size of original and NPFPG copper samples, respectively; and k is a constant related to the material ($k = 0.14 \text{ MPa m}^{1/2}$ for Cu [86]).

For solid solution strengthening, the contribution value of solute elements $\Delta\sigma_{ss} = M\tau_{L-N}$, where $M = 3.06$, τ_{L-N} is the shear stress of solid solution. Generally, the solid solution strengthening model proposed by Labusch and Nabarro is adopted, namely, τ_{L-N} is [87]:

$$\tau_{L-N} = \frac{(2wf_m^4c^2)^{1/3}}{2b^{7/3}(Gb^2)^{1/3}} \quad (6)$$

$$f_m = \frac{Gb^2}{120}\varepsilon_L \quad (7)$$

where b is Burgers vector ($b = 0.25 \text{ nm}$ for Cu) [88], w is the range of the maximum force f_m between a dislocation and a solute atom force ($w = 5$ for Cu) [89], G is the shear modulus ($G = 42.1 \text{ GPa}$ for Cu) [79], and c is the atomic fraction of solute elements; ε_L can be estimated as $12|\varepsilon_b|$, where ε_b is the linear mismatch of solid solution systems such as Cu-Fe, Cu-Co and Cu-Sn. Based on the theoretical calculation, the solubility of iron and cobalt in copper matrix is close to zero at room temperature [44,65,66]. The solid solution atoms of Fe and Co contribute very little to the yield strength of all copper alloy systems, and the predicted values of σ_{ss} are close to 1.2 MPa. The solid solution strengthening in NPFPG copper alloy mainly comes from other components, such as Sn in bronze alloy.

It is generally believed that cracks are generally initiated and propagated in the tin-rich segregation region between dendrites in the tensile fracture process of tin bronze alloy. Figure 14 shows the dendrite outline exposed on the fracture surface of the original Cu-12Sn-1.5Ni alloy, and there are serrated micropores between dendrites. These micropores are caused by the initiation and propagation of cracks in the brittle grain-boundary δ phase, indicating that in the tensile deformation of bronze alloy, cracks tend to preferentially nucleate and propagate at δ phase between dendrites. Therefore, the elimination of coarse segregation δ phase (Figures 4 and 7) in the NPFPG structured bronze alloy is beneficial to the obvious improvement of the ductility. For example, the elongation values of as-cast Cu-10Sn-2Zn-1.5Fe-0.5Co and Cu-12Sn-1.5Ni- x Fe ($x = 0.05\sim 1.5\text{wt.}\%$) alloys are significantly improved relative to the original alloy (Figures 6 and 9).

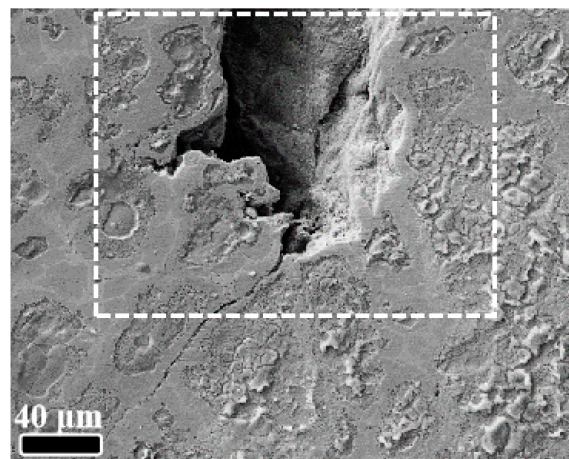


Figure 14. The SEM image of the cross-section of the tensile region around 1 mm beneath the fracture surface of Cu-12Sn-1.5Ni alloy [69].

Unlike NPFPG-Cu, the quantity of grain boundary brittle δ phase in NPFPG structured bronze alloy determines the probability of ductile fracture (transgranular fracture) and brittle fracture (intergranular fracture). The obvious reduction of δ phase in NPFPG structure makes transgranular fracture possible. The cracks initiate and propagate in the brittle δ phase region, and then enters the grain interior. When the crack encounters with iron-rich

nanoparticles, the fresh crack is generated at the interface between iron-rich nanoparticles and copper matrix to realize the crack propagation. In this mode, the smaller the interface bonding force between iron-rich nanoparticles and copper matrix, the interface cracking occurs under smaller applied stress, and eventually leads to the decrease of macroscopic elongation. With the increase of iron content, the size of iron-rich particles increases, which makes the interface fracture between iron-rich particles and copper matrix easier in the tensile deformation process. Therefore, the tin bronze alloy strengthened by small iron-rich nanoparticles show more stable plastic strain and strain hardening rate in the tensile deformation, resulting in the highest ductility.

In general, the yield strength increment of NPFG structured copper alloy mainly comes from the precipitation strengthening of iron-rich nanoparticles. Taking Cu-Fe-Co alloy as an example, as shown in Figure 13b, the Orowan strengthening $\Delta\sigma_{\text{Orowan}}$ of iron-rich nanoparticles dominates the NPFG strengthening effect. Although the contribution of spherical, cuboidal, and petal-like particles is only considered in Figure 13b, the predicted yield strength increment $\Delta\sigma_s$ is in good agreement with the experimental value $\Delta\sigma_s(\text{exp.})$. The results show that the contribution of fully coherent dot-like nanoparticles to precipitation strengthening is very small. Chen et al. [46] roughly predicted the strengthening contribution of dot-like nanoparticles by dislocation shearing mechanism, and obtained the contribution of dot-like nanoparticles to precipitation strengthening is about 2–15 MPa.

With regards to NPFG structure improving plasticity, on the one hand, fine grains provide more grain boundaries to accommodate more dislocations, and more grain boundaries interaction with dislocations to activate more non-basal slip systems. In addition, fine iron-rich nanoparticles provide more nanoparticle-copper matrix interfaces, which accommodate dislocations and activate the non-basal slip system in the process of interaction with dislocations. These two effects improve the plasticity of copper alloy.

3.4. Mechanism of Microstructural Optimization

According to the above microstructural and mechanical results, the strength and ductility of copper alloys reinforced by in-situ iron-rich nanoparticles are greatly improved at the same time, far more than the mechanical properties of their original alloys. A typical microstructure feature of this new alloy is the NPFG structure, that is, a large number of iron-rich nanoparticles are uniformly distributed in the refined micron-sized matrix grains. This microstructure feature is the main reason for the excellent mechanical properties of the alloy. The micron-sized grains ($>1 \mu\text{m}$) in the NPFG structure combined with the iron-rich nanoparticles that were coherent or semi-coherent with the matrix in the grain interior improve the strength without reducing ductility or even improving ductility. More importantly, the NPFG structure in copper alloy is in-situ formed during casting process, which thus can be widely used in mass production of bulk metals and alloys with complex shape. The formation mechanism of NPFG structure has been studied for realizing its wide application.

3.4.1. Mechanism of Grain Refining

First of all, in terms of heterogeneous nucleation mechanism of iron-rich nanoparticles, it is shown that the wettability or lattice matching between the nanoparticles as heterogeneous nucleation substrate and copper matrix, is an important factor affecting the nucleation potential. Moreover, due to the temperature increase of metal melt caused by solidification latent heat, it is required that the particles have a certain size distribution range to ensure the efficiency of inducing nucleation [72,76,90–97]. According to the results of Thermo-Calc and DSC analysis [48], the iron-rich nanoparticles in as-cast Cu-10Sn-2Zn-1.5Fe-0.5Co alloy in-situ precipitate prior to the solidification of copper matrix. The NPFG structured copper alloy is fabricated by electromagnetic induction melting technology, and the alloy was overheated to 1300 °C after melting and held at 1300 °C for 20–30 min. This sufficient time of heat preservation, combined with electromagnetic induction stirring, ensure that Cu, Sn, Fe, and other elements (especially iron elements) are fully mixed and

evenly distributed in the melt, so as to ensure that the iron-rich phase is highly dispersed and precipitated at nanoscale in the melt and matrix of copper alloy during solidification.

Iron-rich nanoparticles first precipitate with f.c.c. structure and cube-on-cube orientation. In terms of thermodynamics, these crystallographic features ensure perfect interface matching to reduce the unique nucleation barrier (i.e., interface energy) in the solidification process, which induce the growth of copper matrix from the surface of iron-rich nanoparticles as the core. Figure 15a,b shows the atomic arrangement on the (111) surface of Cu and γ -Fe, and their crystal orientations $[\bar{1}2\bar{1}]$ and $[0\bar{1}1]$ are marked in the figure [48]. Figure 15c illustrates the nucleation of Cu on iron-rich nanoparticles [48].

To achieve effective grain refinement, particles in the nucleation core need to have high nucleation potential, in other words, the nucleation barrier is low [98]. Turnbull and Vonnegut pointed out that on the premise that the chemical properties of the matrix and nucleated particles are similar, the only nucleation barrier depends on the interface matching between the particles and the matrix [99]. The better lattice matching, the greater nucleation potential [72]. Researchers have proposed the lattice matching conditions that the particles can be used as the core of high potential nucleation [91,92,94–96]: the interatomic misfits between the matrix and the nucleation particles along the matching direction are less than 10%, and the space mismatch between the crystal plane containing the matching direction is less than 6%. The matched crystal planes of the matrix and nucleation particles are usually their close-packed or nearly close-packed planes, and the close-packed planes mostly contain the dense direction of atoms. Therefore, the close-packed direction can be evaluated directly according to the atomic arrangement on the close-packed or nearly close-packed planes.

Wang et al. [48] calculated lattice mismatch values using the cube-on-cube crystal orientation relationship (OR) between iron-rich nanoparticles and matrix in Figure 5. The atomic spacing mismatch along the matching direction (The $[0\bar{1}1]_{\gamma\text{-Fe}}$ orientation on $(111)_{\gamma\text{-Fe}}$ plane and the $[0\bar{1}1]_{\text{Cu}}$ orientation on $(111)_{\text{Cu}}$ plane) is -1.9% , far less than 10%; the crystal plane mismatch between $(111)_{\gamma\text{-Fe}}$ and $(111)_{\text{Cu}}$ is -1.4% , far less than 6%. The (111) crystal plane is the densest arrangement of f.c.c. structural metals. Because of the cube-on-cube OR, the atomic spacing mismatch between γ -Fe and Cu in all matching directions is -1.9% ; the mismatches of other possible matched crystal planes include $(200)_{\gamma\text{-Fe}}$ plane and $(200)_{\text{Cu}}$ plane, $(220)_{\gamma\text{-Fe}}$ plane and $(220)_{\text{Cu}}$ plane, which are -5.3% and -0.79% , respectively, which are calculated by the measured (Figure 5) and the reported crystal plane spacing [100]. It can be seen that the mismatch between the crystal plane of the iron-rich nanoparticles and the matrix, and the mismatch between the atomic spacing on the matching crystal plane, are far less than the threshold to become the high potential nucleation core. The matrix copper can nucleate and grow on the iron-rich nanoparticles with a small interfacial energy barrier. In other words, the iron-rich nanoparticles can be used as a high-potent nucleation core of the matrix copper.

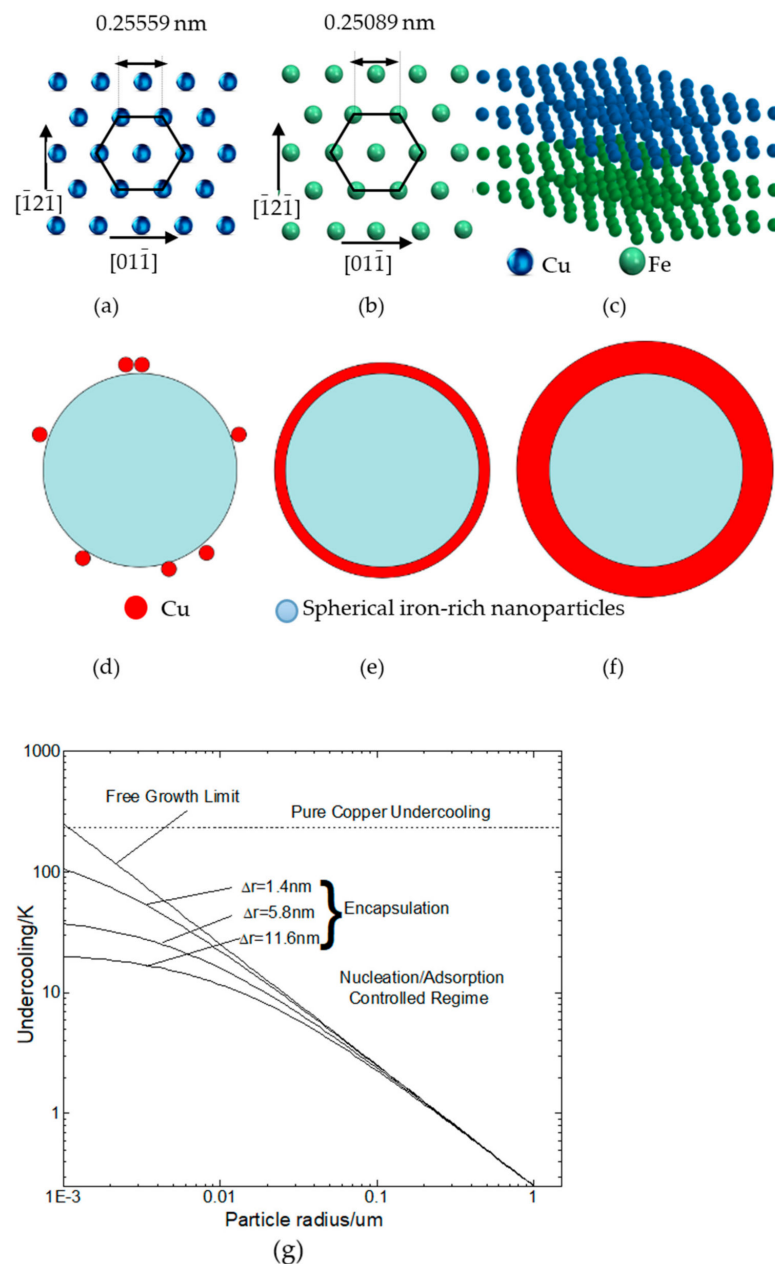


Figure 15. Schematic illustration of the mechanism for adsorption of Cu on (111) surface of an iron-rich nanoparticle: Arrangements of atoms in (a) (111) plane of Cu; (b) Terminated (111) plane of the nanoparticle surface; (c) Atomic matching at the Cu/Fe interface; (d–f) The formation process of encapsulated nanoparticle; (g) The minimum undercooling required for effective nucleation proposed by Greer [48].

From the perspective of wetting, since the iron-rich nanoparticles have the same type of crystal structure and almost the same lattice parameters as the copper matrix in the high-temperature melt, it is reasonable to believe that the crystal surface of the iron-rich nanoparticles can be completely wetted by the copper melt. Therefore, the model proposed by Ma Qian has been used to describe the heterogeneous nucleation process of the copper melt on the iron-rich nanoparticles with high potential [91,93,101]. Spherical iron-rich nanoparticles precipitate early in the melt and suspend in the copper melt. Copper atoms quickly adsorb on the surface of a single spherical iron-rich nanoparticle substrate (Figure 15d); subsequently, a thin layer of copper atom wraps the particle substrate into a core-shell structure (Figure 15e); the copper atomic thin layer continues to grow in the form

of spherical surface, and becomes a thick atomic layer (Figure 15f). Finally, the iron-rich nanoparticles are wrapped by the initial copper atomic layer with different thicknesses and suspended in the copper melt. This kind of nanoparticles wrapped by copper atoms is called encapsulated nanoparticles. The heterogeneous nucleation effect can be predicted by using the relationship model between critical nucleation undercooling ΔT_{crit} and particle size, as shown in Equation (8):

$$\Delta T_{crit} = \frac{0.2533}{r_p(\mu\text{m}) + \Delta r(\mu\text{m})} \quad (8)$$

Equation (8) is derived from the nucleation barrier of spherical substrates with high potential. Beyond this barrier, the subsequent crystal growth process is no longer limited [93]. By substituting the copper thermodynamic parameters into Equation (8), the relation between the critical nucleation undercooling degree ΔT_{crit} of copper melt and the size of encapsulated nanoparticles (including the size of iron-rich nanoparticles r_p and the initial thickness of copper atomic layer Δr) can be obtained. As shown in Figure 15g, for iron-rich nanoparticles with radius less than 220 nm, the copper atomic adsorption layer has a significant indigenous effect on the critical undercooling of nucleation. On the contrary, the nucleation critical undercooling of encapsulated nanoparticles is almost the same as that of the free growth model. According to the experimental observation results of iron-rich nanoparticles in NPFG structured copper alloys (Figures 5, 8 and 11), the size of most nanoparticles is less than the critical value of 220 nm. Therefore, the effect of initial copper atomic layer on the heterogeneous nucleation of encapsulated nanoparticles cannot be ignored.

The copper matrix is randomly heterogeneously nucleated on nanoparticles of different sizes in a certain undercooling range. Figure 15g shows the critical undercooling ΔT_{crit} corresponding to the particle radius r_p between 1 nm~1 μm . Effective nucleation depends on the size of the granular nucleation substrate and the melt undercooling. As mentioned above, iron-rich nanoparticles are uniformly dispersed in copper melt, and only encapsulated nanoparticles with the greatest nucleation potential can preferentially induce copper nucleation. Obviously, ΔT_{crit} increases with the increase of r_p and Δr (see Figure 15g), indicating that the larger encapsulated nanoparticles have greater nucleation potential.

Moreover, the nucleation of copper crystals releases latent heat during the solidification and growth process, which causes the recalescence of the melt and hinder the supercooling required for the nucleation of other encapsulated nanoparticles [71,72]. Thereby, a large part of the encapsulated nanoparticles are not able to induce nucleation. In this context, the original iron-rich nanoparticles with larger r_p and encapsulated nanoparticles with larger $(r_p + \Delta r)$ play a leading role in the process of inducing copper nucleation. Although most of the encapsulated nanoparticles cannot become the core of heterogeneous nucleation, the presence of iron-rich nanoparticles does play an effective role in grain refinement, as shown in Figures 3, 7 and 10.

3.4.2. Capture Mechanism of Iron-Rich Nanoparticles by Solidification Interface

The size distribution of iron-rich nanoparticles is between several nanometers and hundreds of nanometers, and tens of thousands of nanometers, which means that at any undercooling, only part of the encapsulated nanoparticles are activated by heterogeneous nucleation, so the vast majority of encapsulated nanoparticles cannot become the nucleation core [75], which interact with the liquid-solid interface and are captured into the grain during the growth of copper crystals.

Wang et al. [67] used the nanoparticle capture model proposed by J.Q. Xu [14] to explain the capture mechanism of iron-rich nanoparticles in as-cast NPFG structure copper alloy. J.Q. Xu [14] set thermodynamic favorable conditions as the basis for trapping nanoparticles, and discussed the trapping criterion of nanoparticles under the action of three forces. It includes interface energy (solidification interface front range $D = 0.2\sim 0.4$ nm), the van der Waals force (range $D = 0.4\sim 10$ nm), and Brownian force (any position in high

temperature copper melt). For encapsulated nanoparticles, the initial copper atomic layer on the surface reduces the σ_{ps} of the copper-iron system, thus creating thermodynamic favorable conditions for the capture of nanoparticles [14]. As for W_{vdw} , the criterion formula is:

$$W_{vdw}(D) = - \frac{(\sqrt{A_{solid}} - \sqrt{A_{liquid}})(\sqrt{A_{nanoparticle}} - \sqrt{A_{liquid}})}{\left\{ \frac{R}{D} + \frac{R}{2R+D} + \ln \frac{6R}{2R+D} \right\}} \quad (9)$$

where A is the Hamaker constant, an important parameter to evaluate W_{vdw} is positive or negative. Hamaker constant A of high conductive metals can be determined by plasma frequencies of free electrons [14]. It was found from the electron energy loss spectrum of the material that the plasma frequency of Fe was higher than that of Cu [102], indicating that the $A_{nanoparticle}$ in the Cu-Fe system was higher than that of A_{solid} . The plasma frequency of liquid metal is generally higher than that of solid metal [14], so A_{solid} is higher than A_{liquid} . Then, according to the criterion formula of W_{vdw} in Equation (9), the van der Waals force W_{vdw} of encapsulated nanoparticles in copper-iron system is less than zero, which is attractive.

As for the Brownian force, the direction of the Brownian force has the typical characteristics of randomness. Thus, even without the external force interference, the Brownian force always produces the attraction of being captured by the solidification interface as nanoparticles. Therefore, the total interaction force between copper-coated iron nanoparticles and the liquid-solid interface is attractive, and the nanoparticles migrate to the vicinity of the liquid-solid interface (~0.4 nm) and complete the matching with the matrix lattice, so as to realize spontaneous capture. Therefore, all encapsulated nanoparticles are capable to be captured by the liquid-solid interface into the copper crystal and eventually dispersed within the matrix grains to form NPF structure.

3.4.3. Morphological Evolution of Iron-Rich Nanoparticles

An important feature of in-situ iron-rich nanoparticles reinforced NPF copper alloy is the morphology evolution of the nanoparticles from spherical to cuboidal, and to petal-like shapes. The results show that the spherical shape of particles avoid the sharp edges and angles of cubic or petal-like shape, reduce the stress and strain concentration at the sharp interface between particles and matrix during plastic deformation, and alleviate the tendency of producing microcracks at the edges of particles, which improve the ductility of materials [77,103]. For high-temperature service alloys, the morphology of particles evolves in the long-term high-temperature service process, which affects the high-temperature mechanical properties of the alloy in real time [104–106].

Chen et al. [47] studied the morphology evolution behavior of iron-rich nanoparticles in copper alloys in combination with experimental characterization (Figure 11) and phase-field modeling (Figure 16). Results indicated that the morphology evolution of the iron-rich phase occurs in the high temperature copper matrix. Specifically, the f.c.c. iron-rich nanoparticles experienced a spherical → cuboidal → petal-like morphology evolution under the combined effect of interfacial energy, elastic energy, and chemical driving force. Firstly, in the early growth stage (<100 nm), the interface energy plays a dominant role. In order to reduce the interface area or interface energy of Cu-Fe system, the iron-rich nanoparticles formed as spherical shape. Then, the elastic energy becomes a dominant factor with the growth of particle, and the nanoparticles transformed into cuboidal shape to produce “soft” (001) planes. Then, cuboidal nanoparticles with flat interfaces lose stability and become petal-like with concave interfaces. The instability of cuboidal morphology is caused by kinetic factors and depends on the supersaturation around the nanoparticles. In addition, when the distance between nanoparticles is too small, the particles will maintain a cuboidal shape.

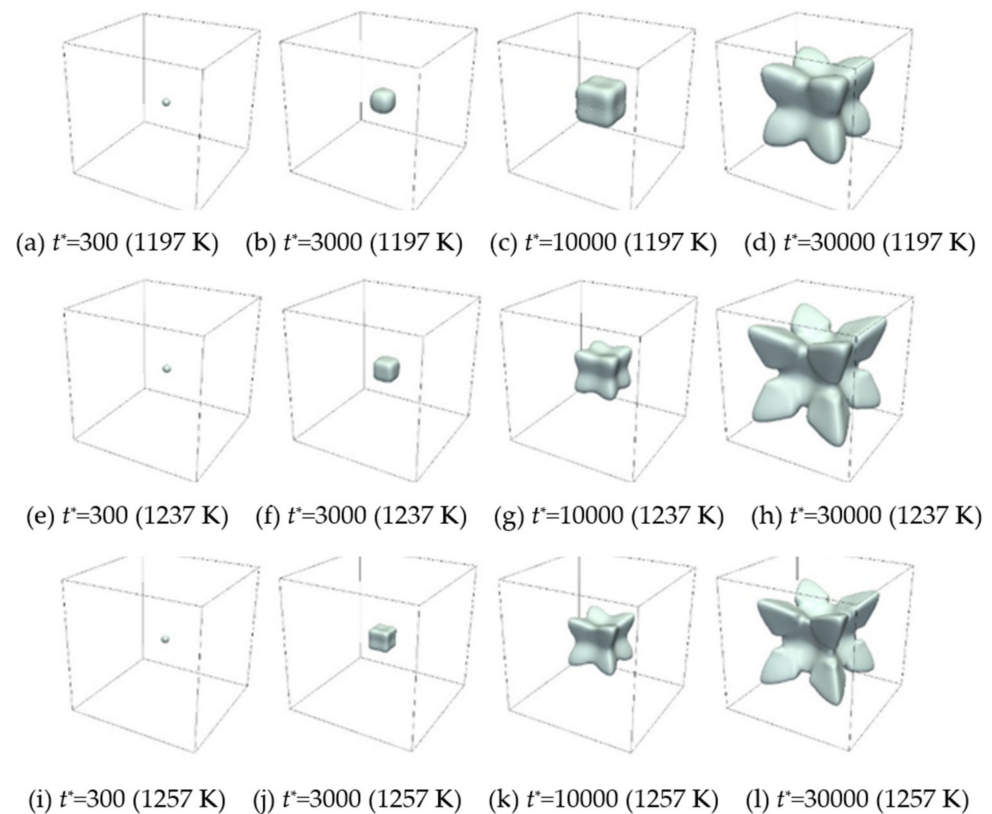


Figure 16. Morphological evolution of the iron-rich single precipitate in Cu-Fe system at different temperatures obtained in phase field modelling. Initial configuration contains an iron pure spherical nucleus of radius $R = 4\Delta x$ [47].

Elastic energy plays different roles in different growth stages of particles. In the early growth stage, the interaction between elastic energy and interface energy promotes the growth of particles along the elastic “soft” orientation. In the late growth stage, elastic energy indirectly affects the cuboidal \rightarrow petal-like transition. The elastic energy only provides a flat particle interface for the transformation, and the chemical driving force ensures the rapid growth of the cuboidal particle corner. It can be expected that the particles with a flat interface in all alloys may be transformed into the shape with a concave interface.

In addition, composition and temperature are important macroscopic factors affecting the morphology evolution of iron-rich particles. The higher the temperature is, the smaller the critical size of the morphology transformation is (Figure 16). The higher iron content, the more obvious coarsening of iron-rich phase, accompanied by the formation of cubic and petal-like morphology [47]. Therefore, in order to control the morphology of iron-rich precipitates and optimize the properties of the alloy, it is necessary to design appropriate temperature and composition to avoid the formation of sharp particles.

3.4.4. Inhibition Mechanism on Tin Segregation

Along with the formation of NPFG structure, the inhibition of tin segregation, which hinders the formation of brittle tin-rich phase at grain boundary, is available in the iron and/or cobalt doped tin bronze alloys. The decrease of δ phase in tin bronze alloy is mainly due to the grain refinement of the alloy, which shortens the path of solute redistribution and weakens the segregation of tin. In addition, the generation of more grain boundaries upon grain refining divides the δ phase and prevents its continuous distribution.

In addition, the addition of different iron content leads to the change of grain refining effect and the change of the weakening degree of grain boundary segregation phase. Taking Cu-12Sn-1.5Ni alloy with different iron content (0, 0.053, 0.63, 1.44 wt.%) as an example,

the increase of iron content leads to the decrease of grain size and the gradual weakening of intergranular coarse continuous brittle δ phase of as-cast Cu-12Sn-1.5Ni alloy (Figure 7).

3.4.5. Section Summary

In view of the above discussion on the formation mechanism of NPFG structure, the interaction between iron-rich nanoparticles and copper matrix during solidification is the main process of in-situ formation of NPFG structure, including the prior precipitation of iron-rich nanoparticles, the formation of copper atomic adsorption layer, the induced nucleation of encapsulated nanoparticles and the spontaneous capture of encapsulated nanoparticles.

The remarkable grain refinement is attributed to the high nucleation potency, appropriate size and size distribution, and adequate number density of iron-rich nanoparticles. The spontaneous capture of encapsulated nanoparticles depends on the high Hamaker constant of iron-rich nanoparticles, and the perfect lattice matching between the nanoparticle and copper matrix. The study on the formation mechanism of NPFG structure provides a potential technological approach for the preparation of bulk NPFG structured copper alloys with excellent mechanical properties. Due to the excellent mechanical properties of as-cast copper alloy with NPFG structure, the analysis of the formation mechanism of NPFG structure opens up a fresh idea for the optimization of microstructure and properties during casting.

4. Conclusions, Gap Analysis and Prospect

In this review, the strengthening methods of metallic materials, especially of copper alloys, are reviewed. Two strengthening methods inclusive of second phase dispersion strengthening and ultrafine-grained strengthening are introduced. Both methods have been widely studied and applied, but are still with problems and shortages. In particular, most of the dispersed second phase strengthening particles applied in industry are the external particles of micron and submicron scales, which cannot overcome the strength-ductility paradox. Although these particles improve the mechanical properties of materials to a certain extent, there are often microstructural problems such as large particle size, easy aggregation, and poor matching relationship with the matrix. In addition, the related preparation processes of the second phase are with high requirements and expensive cost. Furthermore, ultrafine-grained strengthening significantly increases the strength of the material, but always along with the sharp decline in ductility, which cannot solve the contradiction between strength and plasticity either.

In view of the contradiction between strength and plasticity of copper alloy, the concept of NPFG structured copper and copper alloy induced by in-situ nanoprecipitation was introduced. The in-situ preparation, microstructure and mechanical properties of nano-iron-rich precipitation phase reinforced copper and copper alloy were reviewed. Through the appropriate addition of Fe (and/or Co) element and casting technology, a large number of nano-sized iron-rich precipitates are in-situ formed in the conventional solidification process of Cu melt. The iron-rich nanoparticles exhibit good distribution and good compatibility with Cu matrix, and refine the grains of Cu matrix to 1~100 μm along with a significant influence on segregation inhibition. Besides, the finely distributed iron-rich nanoparticles are dispersed in the refined micron-sized grains, and generate the NPFG structure.

Specifically, grain refinement is due to the high efficiency, appropriate size, appropriate size distribution, and sufficient number density of nano-sized precipitates in-situ formed in the melt. Some encapsulated nano-sized precipitates (i.e., iron-rich precipitates encapsulated with the initial copper layer) induce heterogeneous nucleation of copper grains, which promote grain refinement and CET transition, and other encapsulated nano-sized precipitates are incorporated into copper grains by spontaneous capture. The results show that NPFG structured copper and copper alloy not only has optimized microstructure, but also has good comprehensive mechanical response of high ductility and high strength.

Furthermore, four key factors for the preparation of high performance NPFG copper alloys are summarized here. First, nanoparticles meet the thermodynamical conditions of prior precipitation in the melt; second, the crystallographic similarity as well as the minimization of lattice mismatch between nanoparticle and matrix, which favor the enhancement of heterogeneous nucleation potential and the creation of thermodynamic favorable conditions for spontaneous capture process; thirdly, the appropriate casting process and composition, such as induction heating and centrifugal casting, and the control of the addition contents of nanoparticles forming elements, are adopted to promote the appropriate size, morphology, number density, size distribution, and spatial distribution of nanoparticles in the melt, to ensure the high nucleation efficiency and good plasticization effect; fourth, the nanoparticles have a higher Hamaker constant than the matrix, which provides a negative van der Waals force for the spontaneous capture of nanoparticles by solidification interface. Combined with the above key factors, bulk NPFG structured alloy with complex shape, high strength, and high ductility, can be prepared by simple casting process.

It is notable that in-situ nanoparticle strengthening method as well as NPFG idea are expected to become a potential pathway in future industrial mass production for Cu and Cu alloys. However, this method and idea for now are limited in (Fe, Co)-doped Cu alloys, which need to be explored in other Cu alloy systems. In addition, the focus of current research is on as-cast state, and effects of subsequent processing including thermal and deformation treatments on microstructure and performance are still limited and require further investigation to develop further superior properties.

Author Contributions: K.C. and Z.L. wrote the manuscript; K.C., Z.L., Y.Z., J.S. (Jiangxu Shen), and J.S. (Jiayun Shi) conducted a literature survey; Z.W. and X.C. organized the structure of the review article; Z.W., M.C. and Y.W. discussed and commented on the manuscript. All authors have read and agreed to the published version of the manuscript.

Funding: This research was funded by the Beijing Municipal Natural Science Foundation (No. 2214072), the National Natural Science Foundation of China (Grant No. 52101119), the Interdisciplinary Research Project for Young Teachers of USTB (Fundamental Research Funds for the Central Universities, No. FRF-IDRY-20-034), and the Central Funds Guiding the Local Science and Technology Development of Hebei Province (226Z1001G).

Institutional Review Board Statement: Not applicable.

Informed Consent Statement: Not applicable.

Data Availability Statement: Not applicable.

Conflicts of Interest: The authors declare no conflict of interest.

References

1. Lu, K. The future of metals. *Science* **2010**, *328*, 319–320. [[PubMed](#)]
2. Hall, E.O. Deformation and Ageing of Mild Steel: III Discussion of Results. *Proc. Phys. Soc. Lond. Ser. B* **1951**, *64*, 747–753.
3. Petch, N.J. The cleavage of polycrystals. *J. Iron Steel Inst.* **1953**, *174*, 25–28.
4. Huanga, Y.; Langdon, T.G. Advances in ultrafine-grained materials. *Mater. Today* **2013**, *16*, 85–93.
5. Ogut, S.; Kaya, H.; Kentli, A. Comparison of the Effect of Equal Channel Angular Pressing, Expansion Equal Channel Angular Pressing, and Hybrid Equal Channel Angular Pressing on Mechanical Properties of AZ31 Mg Alloy. *J. Mater. Eng. Perf.* **2022**, *31*, 3341–3353.
6. Pourhamid, R.; Shirazi, A. Microstructural evolution and mechanical behaviors of equal channel angular pressed copper. *Proc. Inst. Mech. Part C J. Mech. Eng. Sci.* **2020**, *234*, 171–179.
7. Nuckowski, P.M.; Snopinski, P.; Wrobel, T. Influence of Plastic Strain Accumulation in Continuous Ingots during ECAP on Structure and Recrystallization Temperature of AlCu4MgSi Alloy. *Materials* **2020**, *13*, 576.
8. Machackova, A. Decade of Twist Channel Angular Pressing: A Review. *Materials* **2020**, *13*, 1725.
9. Gupta, A.; Chandrasekhar, B.; Saxena, K.K. Effect of Equal-channel angular pressing on mechanical Properties: An overview. *Mater. Today* **2021**, *45*, 5602–5607.
10. Dong, W.Q.; Zhou, Z.; Zhang, M.D.; Ma, Y.M.; Yu, P.F.; Liaw, P.K.; Li, G. Applications of High-Pressure Technology for High-Entropy Alloys: A Review. *Materials* **2019**, *9*, 867.

11. Figueiredo, R.B.; Horita, Z.; Langdon, T.G. Using High-Pressure Torsion to Achieve Superplasticity in an AZ91 Magnesium Alloy. *Materials* **2020**, *10*, 681.
12. Kalahroudi, F.J.; Koohdar, H.; Sharafutdinov, A.; Jafarian, H.R.; Haung, Y.; Langdon, T.G.; Nili-Ahmadabadi, M. On the microstructure and mechanical properties of an Fe-10Ni-7Mn martensitic steel processed by high-pressure torsion. *Mater. Sci. Eng. A* **2019**, *749*, 27–34.
13. Wang, H.F.; Tang, C.; An, O.G.; Lu, K.; Zhao, Y.H. Microstructure refinement mechanism of undercooled Cu(55)Ni(45) alloys. *Mater. Sci. Pol.* **2021**, *39*, 319–330.
14. Xu, J.Q.; Chen, L.Y.; Choi, H.; Li, X.C. Theoretical study and pathways for nanoparticle capture during solidification of metal melt. *J. Phys. Condens. Matter* **2012**, *24*, 255304.
15. Kushwaha, A.K.; Mishra, A.; Benson John, M.; Misra, M.; Menezes, P.L. Nanocrystalline Materials: Synthesis, Characterization, Properties, and Applications. *Crystals* **2021**, *11*, 1317.
16. Schiøtz, J.; Jacobsen, K.W. A Maximum in the Strength of Nanocrystalline Copper. *Science* **2003**, *301*, 1357–1359.
17. Huang, C.W.; Aoh, J.N. Friction Stir Processing of Copper-Coated SiC Particulate-Reinforced Aluminum Matrix Composite. *Materials* **2018**, *11*, 599.
18. Zhang, G.H.; Mada, T.; Jiang, X.S.; Qiao, C.J.; Shao, Z.Y.; Zhu, D.G.; Zhu, M.H.; Valcarcel, V. Investigation of the Microstructure and Mechanical Properties of Copper-Graphite Composites Reinforced with Single-Crystal-Al₂O₃ Fibres by Hot Isostatic Pressing. *Materials* **2018**, *11*, 982.
19. Lee, J.S.; Jung, J.Y.; Lee, E.S.; Park, W.J.; Ahn, S.; Kim, N.J. Microstructure and properties of titanium boride dispersed Cu alloys fabricated by spray forming. *Mater. Sci. Eng. A* **2000**, *277*, 274–283.
20. Zhang, X.J.; Chen, Z.Q.; Liu, Z.H.; He, M.; Yang, Z.R.; Wang, Z.H. Microstructure and enhanced mechanical properties of ZrC/Zr composites added by in-situ Y₂O₃ reinforced particles. *Vacuum* **2022**, *203*, 111277.
21. Wang, X.; Liu, J.; Zhang, Y.P.; Zhang, A.M.; Hou, H.P.; Zhuang, M.; Du, H.L. Microstructure and mechanical property of novel nanoparticles strengthened AlCrCuFeNi dual-phase high entropy alloy. *Mater. Today* **2022**, *32*, 104155.
22. Li, Z.B.; Zhang, H.; Zhuang, Z.H.; Chou, C.H. Superior strength-ductility synergy in a novel tailored Zr-based particle-strengthened medium W content alloys. *Compos. Part. B* **2022**, *236*, 109817.
23. Wang, Y.; Liu, Z.H.; Zhou, Y.Z.; Yang, X.S.; Tang, J.G.; Liu, X.; Li, J.F.; Le, G.M. Microstructure and mechanical properties of TiN particles strengthened 316L steel prepared by laser melting deposition process. *Mater. Sci. Eng. A* **2021**, *814*, 141220.
24. Yang, X.N.; Cheng, G.G.; Wang, M.L.; Zhao, P. Precipitation and growth of titanium nitride during solidification of clean steel. *J. Univ. Sci. Technol. B* **2003**, *10*, 24–26.
25. Tang, H.; Chen, X.H.; Chen, M.W.; Zuo, L.F.; Hou, B.; Wang, Z.D. Microstructure and mechanical property of in-situ nano-particle strengthened ferritic steel by novel internal oxidation. *Mater. Sci. Eng. A* **2014**, *609*, 293–299.
26. Guan, C.; Chen, G.; Kai, X.Z.; Cao, R.; Miao, C.; Xu, Z.Z.; Zhao, Y.T. Evolution of microstructure and mechanical properties of graphene nanoplates and ZrB₂ nanoparticles reinforced AA6111 composites during hot rolling deformation. *J. Alloys Compd.* **2022**, *920*, 165910.
27. Rashid, M.S. High-strength, low-alloy steels. *Science* **1980**, *208*, 862–869. [[PubMed](#)]
28. Wu, Z.Z.; Duan, B.H.; Wang, D.Z. Effects of shape and size of second phase on mechanical properties of sintered Mo-Y₂O₃ alloys. *Trans. Nonferrous. Met. Soc. China* **2022**, *32*, 1926–1934.
29. Shi, G.D.; Chen, X.H.; Jiang, H.; Wang, Z.D.; Tang, H.; Fan, Y.Q. Strengthening mechanisms of Fe nanoparticles for single crystal Cu-Fe alloy. *Mater. Sci. Eng. A* **2015**, *636*, 43–47.
30. Takata, N.; Ohtake, Y.; Kita, K.; Kitagawa, K.; Tsuji, N. Increasing the ductility of ultrafine-grained copper alloy by introducing fine precipitates. *Scr. Mater.* **2009**, *60*, 590–593.
31. Wang, Z.D.; Wang, X.W.; Wang, Q.S.; Shih, I.; Xu, J.J. Fabrication of a nanocomposite from in-situ iron nanoparticle reinforced copper alloy. *Nanotechnology* **2009**, *20*, 075605. [[PubMed](#)]
32. Chen, X.H.; Wang, Z.D.; Ding, D.; Tang, H.; Qiu, L.L.; Luo, X.; Shi, G.D. Strengthening and toughening strategies for tin bronze alloy through fabricating in-situ nanostructured grains. *Mater. Des.* **2015**, *66*, 60–66. [[CrossRef](#)]
33. Chen, W.; Gao, G.J.; Meng, X.P.; Zhao, X.J.; Jiang, Y.B.; Wang, M.; Li, Z.; Xiao, L.R. Microstructure, properties and strengthening mechanism of Cu-TiB₂-Al₂O₃ composite prepared by liquid phase in-situ reaction casting. *J. Alloys Compd.* **2022**, *912*, 165170.
34. Qin, Y.Q.; Tian, Y.; Peng, Y.Q.; Luo, L.M.; Zan, X.; Xu, Q.; Wu, Y.C. Research status and development trend of preparation technology of ceramic particle dispersion strengthened copper-matrix composites. *J. Alloys Compd.* **2020**, *848*, 156475. [[CrossRef](#)]
35. Yao, L.Y.; Gao, Y.M.; Li, Y.F.; Huang, X.Y.; Wang, Y.R.; Huang, Y.J. Preparation of nanostructural oxide dispersion strengthened (ODS) Mo alloy by mechanical alloying and spark plasma sintering, and its characterization. *Int. J. Refract. Met. Hard Mater.* **2022**, *105*, 105822.
36. Rocky, B.P.; Weinberger, C.R.; Daniewicz, S.R.; Thompson, G.B. Carbide Nanoparticle Dispersion Techniques for Metal Powder Metallurgy. *Metals* **2021**, *11*, 871.
37. Schneibel, J.H.; Liu, C.T.; Hoelzer, D.T.; Mills, M.J.; Hayashi, T.; Wendt, U.; Heyse, H. Development of porosity in an oxide dispersion-strengthened ferritic alloy containing nanoscale oxide particles. *Scr. Mater.* **2007**, *57*, 1040–1043. [[CrossRef](#)]
38. Lu, K.; Lu, L.; Suresh, S. Strengthening Materials by Engineering Coherent Internal Boundaries at the Nanoscale. *Science* **2009**, *324*, 349–352.

39. Liu, Y.G.; Zhang, J.Q.; Tan, Q.Y.; Liu, S.Y.; Li, M.; Zhang, M.X. Additive manufacturing of high strength copper alloy with heterogeneous grain structure through laser powder bed fusion. *Acta Mater.* **2021**, *220*, 117311.
40. Pan, S.W.; Zhou, X.L.; Chen, X.L.; Yang, M.; Cao, Y.D.; Chen, X.H.; Wang, Z.D. In-Situ Nanoparticles: A New Strengthening Method for Metallic Structural Material. *Appl. Sci.* **2018**, *8*, 2479.
41. Gleiter, H. Nanostructured Materials: Basic Concepts and Microstructure. *Acta Mater.* **2002**, *48*, 1–29.
42. Chen, K.X.; Chen, X.H.; Ding, D.; Wang, Z.D. Crystallographic features of iron-rich nanoparticles in cast Cu–10Sn–2Zn–1.5Fe–0.5Co alloy. *Mater. Charact.* **2016**, *113*, 34–42.
43. Wang, Q.S.; Song, Z.F.; Feng, Z.Q.; Wang, Z.D. Microstructure and properties of ZCuSn3Zn8Pb6NiFeCo alloy. *Adv. Mater. Res.* **2012**, *430–432*, 609–618.
44. Chen, K.X.; Chen, X.H.; Wang, Z.D.; Mao, H.H.; Sandström, R. Optimization of deformation properties in as-cast copper by microstructural engineering. Part I. microstructure. *J. Alloys Compd.* **2018**, *763*, 592–605.
45. Chen, K.X.; Pa, S.W.; Zhu, Y.Z.; Cheng, Y.J.; Chen, X.H.; Wang, Z.D. In situ observations of crack propagation in as-cast Cu–1.5Fe–0.5Co (wt%) alloy. *Mater. Sci. Eng. A* **2017**, *706*, 211–216.
46. Chen, K.X.; Pan, S.H.; Chen, X.H.; Wang, Z.D.; Sandström, R. Optimisation of deformation properties in as-cast copper by microstructural engineering. Part II. Mechanical properties. *J. Alloys Compd.* **2020**, *812*, 151910.
47. Chen, K.X.; Korzhavyi, P.A.; Demange, G.; Zapolsky, H.; Patte, R.; Boisse, J.; Wang, Z.D. Morphological instability of iron-rich precipitates in Cu-Fe-Co alloys. *Acta Mater.* **2019**, *163*, 55–67.
48. Chen, K.X.; Chen, X.H.; Ding, D.; Shi, G.D.; Wang, Z.D. Formation mechanism of in-situ nanostructured grain in cast Cu–10Sn–2Zn–1.5Fe–0.5Co (wt.%) alloy. *Mater. Des.* **2016**, *94*, 338–344.
49. Chen, K.X.; Chen, X.H.; Ding, D.; Shi, G.D.; Wang, Z.D. Heterogeneous nucleation effect of in situ iron-rich nanoparticles on grain refinement of copper alloy. *Mater. Lett.* **2016**, *168*, 188–191.
50. Chen, K.X.; Zhang, J.W.; Chen, Y.J.; Chen, X.H.; Wang, Z.D.; Sandström, R. Slow strain rate tensile tests on notched specimens of as-cast pure Cu and Cu-Fe-Co alloys. *J. Alloys Compd.* **2020**, *822*, 153647.
51. Neikov, O.D.; Naboychenko, S.S.; Murashova, I.B. *Handbook of Non-Ferrous Metal Powders*; Elsevier Science: Amsterdam, The Netherlands, 2009; pp. 331–368. ISBN 978-1-85617-422-0.
52. Zhao, M.; Xu, B.Y.; Zhang, P.; Xu, J.J.; Jiang, Y.; Liu, F.; Yan, Y.W. Microstructure development of Y-Ti-O dispersion strengthened Cu alloys fabricated by mechanical alloying. *Mater. Charact.* **2022**, *186*, 111808. [[CrossRef](#)]
53. Shen, K.; Wang, M.P.; Li, S.M. Study on the properties and microstructure of dispersion strengthened copper alloy deformed at high temperatures. *J. Alloys Compd.* **2009**, *479*, 401–408. [[CrossRef](#)]
54. Geng, Y.F.; Ban, Y.J.; Song, K.X.; Zhang, Y.; Tian, B.H.; Liu, Y. A review of microstructure and texture evolution with nanoscale precipitates for copper alloys. *J. Mater. Res. Technol.* **2020**, *9*, 11918–11934. [[CrossRef](#)]
55. Danninger, H.; Mayer, C.G. *Advances in Powder Metallurgy*; Woodhead Publishing: Cambridge, UK; Sawston, UK, 2013; pp. 149–201. ISBN 978-0-85709-420-9.
56. Hu, Y.S.; Hu, Z.Y.; Fan, G.L.; Tan, Z.Q.; Zhou, Z.D.; Zhang, H.; Li, Z.Q. Simultaneous enhancement of strength and ductility with nano dispersoids in nano and ultrafine grain metals: A brief review. *Rev. Adv. Mater. Sci.* **2020**, *59*, 352–360. [[CrossRef](#)]
57. Chinh, N.Q.; Kovacs, Z. Unique microstructural and mechanical properties of Al-Zn alloys processed by high-pressure torsion. *Mater. Sci. Eng.* **2019**, *613*, 012028. [[CrossRef](#)]
58. Lowe, T.C.; Zhu, Y.T.; Semiati, S.L.; Berg, D.R. Overview and outlook for materials processed by severe plastic deformation. In *Investigations and Applications of Severe Plastic Deformation*; Springer: Berlin/Heidelberg, Germany, 2000; p. 347.
59. Wu, B.; Fu, H.; Qian, L.; Luo, J.S.; Lee, W.B.; Yang, X.S. Severe plastic deformation-produced gradient nanostructured copper with a strengthening-softening transition. *Mater. Sci. Eng. A* **2021**, *819*, 141495. [[CrossRef](#)]
60. Segal, V.M. Materials processing by simple shear. *Mater. Sci. Eng. A* **1995**, *197*, 157–164. [[CrossRef](#)]
61. Valiev, R.Z.; Langdon, T.G. Principles of equal-channel angular pressing as a processing tool for grain refinement. *Prog. Mater. Sci.* **2006**, *51*, 881–981. [[CrossRef](#)]
62. Jiang, S.H.; Wang, H.; Wu, Y.; Liu, X.J.; Chen, H.H.; Yao, M.J.; Gault, B.; Ponge, D.; Raabe, D.; Hirata, A.; et al. Ultrastrong steel via minimal lattice misfit and high-density nanoprecipitation. *Nature* **2017**, *544*, 460–464. [[CrossRef](#)]
63. Yang, T.; Zhao, Y.L.; Tong, Y.; Jiao, Z.B.; Wei, J.; Cai, J.X.; Han, X.D.; Chen, D.; Hu, A.; Kai, J.J.; et al. Multicomponent intermetallic nanoparticles and superb mechanical behaviors of complex alloys. *Science* **2018**, *362*, 933–937. [[CrossRef](#)]
64. Peng, S.; Wei, Y.; Gao, H. Nanoscale precipitates as sustainable dislocation sources for enhanced ductility and high strength. *Proc. Natl. Acad. Sci. USA* **2020**, *117*, 5204–5209. [[CrossRef](#)] [[PubMed](#)]
65. Dong, Q.; Shen, L.; Cao, F.; Jia, Y.; Wang, M. Study of the coarsening and hardening behaviors of coherent α -Fe particles in Cu–2.1Fe alloy. *Acta Metall. Sin.* **2014**, *50*, 1224–1230.
66. Guo, C.J.; Wan, J.; Chen, J.H.; Xiao, X.P.; Huang, H.; Liu, J.P. Inhibition of discontinuous precipitation and enhanced properties of Cu–15Ni–8Sn alloy with Fe addition. *Mater. Sci. Eng. A* **2020**, *795*, 139917. [[CrossRef](#)]
67. Chen, K.X.; Chen, X.H.; Wang, Z.D. Precipitates-interaction capture of nano-sized iron-rich precipitates during copper solidification. *Mater. Sci. Tech. Lond.* **2019**, *35*, 1743–2847. [[CrossRef](#)]
68. Chen, K.X.; Chen, X.H.; Ding, D.; Wang, Z.D. Effect of in-situ nanoparticle wall on inhibiting segregation of tin bronze alloy. *Mater. Lett.* **2016**, *175*, 148–151. [[CrossRef](#)]

69. Chen, K.X.; Zhang, J.W.; Chen, X.H.; Ding, D.; Wang, Z.D.; Shi, R.J.; Zhang, A.J. The effect of iron on the microstructure and mechanical properties of a cast Cu–12Sn–1.5Ni (wt. %) alloy. *Mater. Sci. Eng. A* **2020**, *785*, 139330. [[CrossRef](#)]
70. Chen, Z.N.; Kang, H.J.; Fan, G.H.; Li, J.H.; Lu, Y.P.; Jie, J.C.; Zhang, Y.B.; Li, T.J.; Jian, X.G.; Wang, T.M. Grain refinement of hypoeutectic Al–Si alloys with B. *Acta Mater.* **2016**, *120*, 168–178. [[CrossRef](#)]
71. Ren, L.; Zhang, S.R.; Shi, J.Q.; Shen, Z.; Shi, P.Z.; Zheng, T.X.; Ding, B.; Guo, Y.F.; Zhong, Y.B. Grain refinement and mechanical properties enhancement of Cu–10 wt%Fe alloys via Zr addition. *Mater. Sci. Eng. A* **2022**, *864*, 143309. [[CrossRef](#)]
72. Zhao, K.; Gao, T.; Yang, H.B.; Hu, K.Q.; Liu, G.L.; Sun, Q.Q.; Nie, J.F.; Liu, X.F. Enhanced grain refinement and mechanical properties of a high-strength Al–Zn–Mg–Cu–Zr alloy induced by TiC nano-particles. *Mater. Sci. Eng. A* **2021**, *806*, 140852. [[CrossRef](#)]
73. Zhang, D.Y.; Qiu, D.; Gibson, M.A.; Zheng, Y.F.; Fraser, H.L. Additive manufacturing of ultrafine-grained high-strength titanium alloys. *Nature* **2019**, *576*, 91–95. [[CrossRef](#)]
74. Maxwell, I.; Hellawell, A. An analysis of the peritectic reaction with particular reference to Al–Ti alloys. *Acta Metall.* **1975**, *23*, 229–237. [[CrossRef](#)]
75. GREER, A.L.; Bunn, A.M.; Tronche, A.; Evans, P.V.; Bristow, D.J. Modelling of inoculation of metallic melts: Application to grain refinement of Aluminium by Al–Ti–B. *Acta Mater.* **2000**, *48*, 2823–2835. [[CrossRef](#)]
76. Tian, Y.Z.; Zhao, L.J.; Park, N.; Liu, R.; Zhang, P.; Zhang, Z.J.; Shibata, A.; Zhang, Z.F.; Tsuji, N. Revealing the deformation mechanisms of Cu–Al alloys with high strength and good ductility. *Acta Mater.* **2016**, *110*, 61–72. [[CrossRef](#)]
77. Qin, S.Y.; Chen, C.R.; Zhang, G.D.; Wang, W.L.; Wang, Z.G. The effect of particle shape on ductility of SiCp reinforced 6061 Al matrix composites. *Mater. Sci. Eng. A* **1999**, *272*, 363–370. [[CrossRef](#)]
78. Han, S.Z.; Kim, K.H.; Kang, J.; Joh, H.; Kim, S.M.; Ahn, J.H.; Lee, J.; Lim, S.H.; Han, B. Design of exceptionally strong and conductive Cu alloys beyond the conventional speculation via the interfacial energy-controlled dispersion of γ -Al₂O₃ nanoparticles. *Sci. Rep.* **2015**, *5*, 17364.
79. Kumar, N.; Choudhuri, D.; Banerjee, R.; Mishra, R.S. Strength and ductility optimization of Mg–Y–Nd–Zr alloy by microstructural design. *Int. J. Plast.* **2015**, *68*, 77–97. [[CrossRef](#)]
80. Yuan, S.P.; Liu, G.; Wang, R.H.; Zhang, G.J.; Pu, X.; Sun, J.; Chen, K.H. Aging-dependent coupling effect of multiple precipitates on the ductile fracture of heat-treatable aluminum alloys. *Mater. Sci. Eng. A* **2009**, *499*, 387–395. [[CrossRef](#)]
81. Guo, Z.K.; Jie, G.C.; Liu, J.M.; Yue, S.P.; Liu, S.C.; Li, T.J. Effect of cold rolling on aging precipitation behavior and mechanical properties of Cu–15Ni–8Sn alloy. *J. Alloys Compd.* **2020**, *848*, 156275. [[CrossRef](#)]
82. Martin, J.W. *Precipitation Hardening*, 2nd ed.; Butterworth-Heinemann: Oxford, UK, 1998; pp. 1–125.
83. Ardell, A.J. Precipitation Hardening. *Metall. Trans. A* **1985**, *16*, 2131–2165. [[CrossRef](#)]
84. Gazizov, M.; Kaibyshev, R. Precipitation structure and strengthening mechanisms in an Al–Cu–Mg–Ag alloy. *Mater. Sci. Eng. A* **2017**, *702*, 29–40. [[CrossRef](#)]
85. Cheng, J.Y.; Tang, B.B.; Yu, F.X.; Shen, B. Evaluation of nanoscaled precipitates in a Cu–Ni–Si–Cr alloy during aging. *J. Alloys Compd.* **2014**, *614*, 189–195. [[CrossRef](#)]
86. Rajkovic, V.; Bozic, D.; Stasic, J.; Wang, H.W.; Jovanovic, M.T. Processing, characterization and properties of copper-based composites strengthened by low amount of alumina particles. *Powder Technol.* **2014**, *268*, 392–400. [[CrossRef](#)]
87. Zander, J.; Sandström, R.; Vitos, L. Modelling mechanical properties for non-hardenable aluminium alloys. *Comp. Mater. Sci.* **2007**, *41*, 86–95. [[CrossRef](#)]
88. Correia, J.B.; Davies, H.A.; Sellars, C.M. Strengthening in rapidly solidified age hardened Cu–Cr and Cu–Cr–Zr alloys. *Acta Mater.* **1997**, *45*, 177–190. [[CrossRef](#)]
89. Koike, J.; Kobayashi, T.; Mukai, T.; Watanabe, H.; Suzuki, M.; Maruyama, K.; Higashi, K. The activity of non-basal slip systems and dynamic recovery at room temperature in fine-grained AZ31B magnesium alloys. *Acta Mater.* **2003**, *51*, 2055–2065. [[CrossRef](#)]
90. Ng, K.L.; Sasaki, H.; Kimura, H.; Yoshikawa, T.; Maeda, M. Heterogeneous Nucleation of Graphite on Rare Earth Compounds during Solidification of Cast Iron. *ISIJ Int.* **2018**, *58*, 123–131. [[CrossRef](#)]
91. Shu, S.P.; Wells, P.B.; Almirall, N.; Odette, G.R.; Morgan, D.D. Thermodynamics and kinetics of core-shell versus appendage co-precipitation morphologies: An example in the Fe–Cu–Mn–Ni–Si system. *Acta Mater.* **2018**, *157*, 298–306. [[CrossRef](#)]
92. Qian, M. Heterogeneous nucleation on potent spherical substrates during solidification. *Acta Mater.* **2007**, *55*, 943–953. [[CrossRef](#)]
93. Zhang, M.X.; Kelly, P.M.; Qian, M. Crystallography of grain refinement in Mg–Al based alloys. *Acta Mater.* **2005**, *53*, 3261–3270. [[CrossRef](#)]
94. Fan, Z.; Gao, F.; Wang, Y.; Men, H.; Zhou, L. Effect of solutes on grain refinement. *Prog. Mater. Sci.* **2022**, *123*, 100809. [[CrossRef](#)]
95. Park, S.B. Heterogeneous nucleation models to predict grain size in solidification. *Prog. Mater. Sci.* **2022**, *123*, 100822. [[CrossRef](#)]
96. Quested, T.E.; Greer, A.L. The effect of the size distribution of inoculant particles on as-cast grain size in aluminium alloys. *Acta Mater.* **2004**, *52*, 3859–3868. [[CrossRef](#)]
97. Chen, X.R.; Jia, Y.H.; Le, Q.C.; Ning, S.C.; Li, X.Q.; Yu, F.X. The interaction between in situ grain refiner and ultrasonic treatment and its influence on the mechanical properties of Mg–Sm–Al magnesium alloy. *J. Mater. Res. Technol.* **2020**, *9*, 9262–9270. [[CrossRef](#)]
98. Fan, Z.; Wang, Y.; Xia, M.; Arumuganathar, S. Enhanced heterogeneous nucleation in AZ91D alloy by intensive melt shearing. *Acta Mater.* **2009**, *57*, 4891–4901. [[CrossRef](#)]
99. Turnbull, D.; Vonnegut, B. Nucleation catalysis. *Ind. Eng. Chem.* **1952**, *44*, 1292–1298. [[CrossRef](#)]

100. Zhou, Y.; Wu, G.H. *Analysis Methods in Materials Science: X-ray Diffraction and Electron Microscopy IN Materials Science*; Harbin Institute of Technology Press: Harbin, China, 2007.
101. Kim, W.T.; Cantor, B. An adsorption model of the heterogeneous nucleation of solidification. *Acta Metall. Mater.* **1994**, *42*, 3115–3127. [[CrossRef](#)]
102. Egerton, R.F. *Electron Energy-Loss Spectroscopy in the Electron Microscope*, 3rd ed.; Springer: New York, NY, USA, 2011.
103. Böhm, H.J.; Rasool, A. Effects of particle shape on the thermoelastoplastic behavior of particle reinforced composites. *Int. J. Solids Struct.* **2016**, *87*, 90–101. [[CrossRef](#)]
104. Shan, L.Y.; Li, Y.; Wang, Y.P. Improving the high temperature mechanical performance of Cu-Cr alloy induced by residual nano-sized Cr precipitates. *Mater. Sci. Eng. A* **2022**, *845*, 143250. [[CrossRef](#)]
105. Xu, R.F.; Geng, Z.W.; Wu, Y.Y.; Chen, C.; Ni, M.; Li, D.; Zhang, T.M.; Huang, T.M. Microstructure and mechanical properties of in-situ oxide-dispersion-strengthened NiCrFeY alloy produced by laser powder bed fusion. *Adv. Pow. Mater.* **2022**, *1*, 100056. [[CrossRef](#)]
106. Yusuke, S.; Masataka, M.; Kenta, Y.; Yasuyoshi, N.; Toyokiho, J.K. Microstructural changes of oxide dispersion strengthened copper powders fabricated by mechanical alloying. *Fus. Eng. Des.* **2021**, *173*, 112804.